OHSTPY-HEP-T-96-019
hep-ph/9612291
October 1996

arXiv:hep-ph/9612291v2 25 Mar 1997

PERTURBATIVE QCD AT HIGH TEMPERATURE[1]

AGUSTIN NIETO
Department of Physics, The Ohio State University
Columbus, OH 43210, USA

Abstract

Recent developments of perturbation theory at finite temperature based on effective field theory methods are reviewed. These methods allow the contributions from the different scales to be separated and the perturbative series to be reorganized. The construction of the effective field theory is shown in detail for ϕ^4 theory and QCD. It is applied to the evaluation of the free energy of QCD at order g^5 and the calculation of the g^6 term is outlined. Implications for the application of perturbative QCD to the quark-gluon plasma are also discussed.

[1]Published in *Int.J.Mod.Phys.* A **12**, 1431 (1997)

1 Introduction

In this paper I review some of the recent developments in perturbative field theory at finite temperature that have come about by using effective field theory methods. In particular, we will be interested in the behavior of hadronic matter at high temperature. This means that the temperature is assumed to be much larger than the mass of the particles involved ($T \gg m$). Another assumption is that the gauge coupling constant g is small ($g \ll 1$); this allows us to define three energy scales that satisfy: $T \gg gT \gg g^2T$. Hadronic matter is expected to undergo a phase transition when $T \sim T_c \simeq 200$ MeV between a low temperature phase in which it is confined in the form of hadrons and a high temperature phase in which quarks and gluons are deconfined. The latter phase, known as *Quark-Gluon Plasma* (QGP), can be studied by perturbative methods since the strong coupling constant $\alpha_s(T)$ is expected to be small at high temperature. Later on, we will check the validity of this statement; it happens that at temperatures of a few times T_c, the strong coupling constant is not small enough to give rise to a convergent series in the case of the free energy.

A field theory at high temperature may be described by a lagrangian in which the modes with zero Matsubara frequency have been decoupled according to the Appelquist-Carazzone theorem [1]. Since the resulting theory is 3-dimensional, this method is know as dimensional reduction [2, 3, 4]. An efficient approach consists of interpreting the dimensionally reduced theory as an effective field theory [5] whose parameters are to be computed as a perturbative expansion in the coupling constant of the original theory. This idea is very attractive when studying theories with fermions on the lattice: the dimensionally reduced theory does not contain fermions because they have been integrated out completely and this may simplify computer simulations [6]. The parameters of the effective theory can be determined by analytic methods.

Effective field theory methods have been applied to different problems. Braaten [7] has resolved a longstanding problem involving the breakdown of the perturbation expansion for the free energy of QCD. Braaten and Nieto have determined the asymptotic behavior of the correlator of Polyakov loops [8]. They have also used this method to carry out explicit calculations in ϕ^4 [9] and in QCD [10, 11]. The problem of the finite T electroweak phase transition has essentially been solved in [12]; this work has recently been reviewed by Shaposhnikov in an article [13] that is complementary to this review. Andersen [14] has analytically computed the free energy of QED up to order e^5 and the electric screening mass of scalar QED up to order e^4. Arnold and Yaffe [15] have proposed a rigorous nonperturbative definition of the Debye screening mass in nonabelian gauge theories. Recently, Karsch *et al.* [16] have computed the nonperturbative contribution to the g^6-order term of the free energy of QCD [7, 11] by using lattice simulations. Also, the effective field theory approach has been applied to the study of the Minimal Supersymmetric Standard Model [17].

The effective field theory approach is now a well-established perturbative method to study field theories at finite temperature. It is a useful tool for organizing calculations of high-order terms in the perturbation expansion and it is especially powerful in dealing with nonabelian gauge theories. It is also an important conceptual tool that explicitly separates the different energy scales. In this review I present some of the results of its application to QCD. There are two conceptual steps: first, the effective field theory is defined by computing its parameters by matching with the original theory; second, the effective theory is used to

study problems concerning the high temperature limit of the full theory.

We will use dimensional reduction to construct an effective field theory of QCD whose parameters encode the physics from the scale T; this theory is called *Electrostatic QCD* (EQCD), because it consists of pure Yang-Mills in three dimensions plus a scalar field in the adjoint representation which is related to the static mode of the original chromelectric field. Since, the effective mass of the scalar is of order gT and magnetostatic fields remain massless, we can use the decoupling theorem to construct another effective theory in which the scalar field is decoupled. We will end up with a pure Yang-Mills theory in three dimensions that is called *Magnetostatic QCD* (MQCD) because it is only made out of fields related to the magnetostatic modes of QCD; its parameters encode the physics from the scale gT. In both EQCD and MQCD, the effective lagrangian includes an infinite series of nonrenormalizable terms. One of the technically more involved problems in constructing the effective field theory is the evaluation of Feynman diagrams. In what follows I will not give details of these calculations, I will just state the results of the integrals that are needed and give references, which are basically the appendices in [9, 11]. In all other respects I will try to show the construction of the effective theory in detail.

The next section reviews some concepts that are familiar in the context of quantum field theory at finite temperature (more information can be found in the textbooks [18, 19]), introduces the effective field theory approach for ϕ^4 theory, and shows a complete calculation using its effective field theory. In Sect. 3, the contributions to the QCD free energy from the relevant scales are separated. Sect. 4 is devoted to the construction of EQCD. The free energy of QCD is explicitly computed in Sect. 5 up to order g^5; also the result at order g^6 is analyzed. In Sect. 6 we will study the convergence of the perturbative series for the free energy. Conclusions and final comments are given in Sect. 7.

2 Field Theory at Finite Temperature

The static properties of a system of particles in thermal equilibrium at temperature T are obtained from the free energy density

$$F = -\frac{T}{V} \log \mathcal{Z} \,, \tag{1}$$

where $\mathcal{Z}$ is the partition function. All through this paper, we will use the imaginary-time formalism which is more suitable than the real-time formalism for studying static properties. The partition function of a theory for a field Φ is, in general, of the form

$$\mathcal{Z}(\beta) = \int \mathcal{D}\Phi(\mathbf{x},\tau) \exp\left\{ -\int_0^\beta d\tau \int d\mathbf{x}\, \mathcal{L}(\Phi) \right\} , \tag{2}$$

where τ is the Euclidean time and $\beta = 1/T$. Also, Φ satisfies periodic boundary conditions in τ if it represents a bosonic field or anti-periodic boundary conditions if it represents a fermionic field:

$$\Phi(\mathbf{x},0) = \pm \Phi(\mathbf{x},\beta) \,. \tag{3}$$

These conditions allow us to expand Φ in its Fourier modes:

$$\Phi(\mathbf{x},\tau) = T \sum_n \phi_n(\mathbf{x}) e^{i\omega_n \tau} \,. \tag{4}$$

The Matsubara frequency of the nth mode is $\omega_n = (2n)\pi T$ for bosons and $\omega_n = (2n+1)\pi T$ for fermions. The term in (4) with $\omega_n = 0$ is independent of the Euclidean time τ. The mode with this zero Matsubara frequency is called *static*; the rest of the modes involve τ and are called *nonstatic*.

The Feynman rules are the same as in the Euclidean field theory, except that, at finite temperature, the time-like component of the momentum is discrete: $K^\mu = (\omega_n, \mathbf{k})$. Consequently, the loop integration over such a component is replaced by a sum and the rule for loops is

$$\not{\int}_K \equiv \left(\frac{e^\gamma \mu^2}{4\pi}\right)^\epsilon T \sum_{K_0=\omega_n} \int \frac{d^{3-2\epsilon}k}{(2\pi)^{3-2\epsilon}}\,, \tag{5}$$

where $3-2\epsilon$ is the dimension of the space and μ is an arbitrary renormalization scale. The factor $(e^\gamma/4\pi)^\epsilon$ is introduced so that, after minimal subtraction of the poles in ϵ due to ultraviolet divergences, μ coincides with the renormalization scale in the $\overline{\rm MS}$ renormalization scheme.

For example, in the ϕ^4 theory with a massless scalar field and interaction $g^2\Phi^4$, described by the lagrangian

$$\mathcal{L} = \frac{1}{2}(\partial\Phi)^2 + \frac{g^2}{4!}\Phi^4\,, \tag{6}$$

the leading-order contribution to the self-energy for a particle of momentum $P^\mu = (E_n, \mathbf{p})$ is given by the tadpole diagram in Fig. 1(a):

$$\Pi^{(1)}(P) = \frac{g^2}{2}\not{\int}_K \frac{1}{K^2} = \frac{g^2T^2}{24}\,, \tag{7}$$

where $K^2 = \omega_n^2 + k^2$.

If we try to compute the next-order correction to the self-energy which is given by the Fig. 1(b), we will find out that it is infrared divergent. The same is true for the rest of the diagrams shown in Fig. 1. This *mild* breakdown of the perturbative expansion may be cured by resumming the geometric series of diagrams with one-loop-tadpole insertions like those in the Fig. 1. The result is finite and gives the self-energy at next-to-leading order in g:

$$\Pi = \frac{g^2}{2}\not{\int}_K \frac{1}{K^2 + \Pi^{(1)}} = \frac{g^2T^2}{24}\left(1 - \frac{\sqrt{6}}{4\pi}g + \mathcal{O}(g^2)\right)\,. \tag{8}$$

The sum-integral may be found in [20]. We see that the perturbative series is not analytic in the coupling constant g^2, but in g. This is a general feature of the resummation of diagrams with insertions of the leading-order contribution of the self-energy.

Ultraviolet divergences are not a special issue at finite temperature. The very same counterterms that would regularize the theory at zero temperature regularize the finite temperature theory. This can be understood by realizing that a theory at finite temperature is defined in a 4-dimensional Euclidean space whose time component is compactified into a circle of circumference $1/T$. The short-distance behavior is not modified by this sort of compactification.

2.1 Dimensional Reduction

Let us consider the Appelquist-Carazzone decoupling theorem for a field theory at zero temperature. It states that for a renormalizable field theory with heavy fields (let us say, with mass $\sim M$) and light fields (with mass $\sim m \ll M$), Green's functions with typical momentum scale $p \ll M$ and that only involve light fields in the external legs may be computed without considering heavy field loops. Up to corrections suppressed by powers of p/M and m/M, such Green's functions are described by the original lagrangian with the heavy fields removed, but with modified values for the coupling constants of the light fields. In this sense, the heavy fields decouple from the light fields.

The partition function of a field theory at finite T may be written in terms of the Fourier modes $\phi_n(\mathbf{x})$, defined in (4), instead of $\Phi(\mathbf{x}, \tau)$:

$$\mathcal{Z} = \int \mathcal{D}\phi_0(\mathbf{x}) \mathcal{D}\phi_n(\mathbf{x}) \exp\left\{ - \int_0^\beta d\tau \int d\mathbf{x}\, \mathcal{L}(\phi_0, \phi_n, \tau) \right\} . \tag{9}$$

A propagator of the form $1/(\omega_n^2 + k^2)$ can be associated with each mode and the corresponding Matsubara frequency represents its mass. In this context, all of the fermionic modes and the nonstatic bosonic modes have a mass of order T, while the static bosonic modes are massless.

In the limit of high temperature, nonstatic modes have a large mass of order T when compared with static modes, which are massless; therefore, the decoupling theorem suggests that they decouple. What remains is an effective theory of the static modes whose partition function is of the form

$$\mathcal{Z} = \int \mathcal{D}\phi(\mathbf{x}) \exp\left\{ - \int d\mathbf{x}\, \mathcal{L}_{\text{eff}}(\phi) \right\} , \tag{10}$$

where $\phi(\mathbf{x}) \equiv \sqrt{T}\phi_0(\mathbf{x})$ and $\mathcal{L}_{\text{eff}}$ is the effective lagrangian. The effective theory is defined in a 3 dimensional space; this is why this procedure is known as *dimensional reduction*. Note that all fermionic modes have masses of order T and therefore are integrated out. There are no effective fields associated with them. Their effects are all incorporated into the effective theory through the effective coupling constants for the bosonic modes.

There is an important difference between the decoupling theorem applied to heavy fields at zero temperature and to dimensional reduction at high temperature [4]. For heavy fields at zero temperature, the effective theory is usually taken to be renormalizable. It reproduces Green's functions of the full theory to all orders in the coupling constant g, up to corrections that fall like powers of p/M and m/M. It is possible to reproduce these corrections as well but only at the cost of introducing nonrenormalizable terms into the effective lagrangian. As we have seen for the $g^2\Phi^4$ theory at high temperature, perturbative corrections generate a mass m for the field of order gT, while the nonstatic field has a mass M of order T. The renormalizable effective theory provided by the decoupling theorem reproduces Green's functions only up to errors that fall like powers of m/M, but in this case the errors correspond to powers of g. Thus the renormalizable theory does not reproduce the full theory to all orders in g. Landsman [21] has concluded that the validity of the decoupling theorem at finite T depends on the theory under study and fails for QCD or ϕ^4 theory. This is true only if dimensional reduction is taken in the restricted sense of reducing to a renormalizable effective theory. As in the case of heavy fields at zero temperature, corrections that fall like

powers of m/M can be reproduced by including nonrenormalizable terms in the effective theory.

The effective lagrangian therefore has an infinite number of interaction terms; only a few of them are renormalizable, while the rest are non-renormalizable. Each term has a parameter that plays the role of an effective coupling constant. These parameters are not arbitrary coefficients but instead are completely determined by the condition that the effective theory matches the full theory at low momentum. These effective parameters can be calculated in powers of the coupling constant g of the full theory. Also, in general, the effective parameters depend on an ultraviolet cutoff that cancels the ultraviolet cutoff dependence of the loop integrals in the effective theory. In calculations of a physical quantity to a given order in g, only a finite number of these parameters will enter. At low orders in g, it is sometimes possible to truncate the effective theory to the renormalizable terms or even to the super-renormalizable terms.

2.2 A nontrivial example: the screening mass of ϕ^4 theory

In this subsection we will explicitly construct the effective field theory of a massless field with self-interaction $g^2\Phi^4$ described by the lagrangian (6) and apply it to evaluate the screening mass.

In QED, the electric screening mass describes the asymptotic behavior of the potential between two static charges at large distances. The potential is

$$V(R) = \int \frac{d^3k}{(2\pi)^3} \, \frac{e^{-i\mathbf{k}\cdot\mathbf{R}}}{k^2 + \Pi_{00}(0,\mathbf{k})} \,, \tag{11}$$

where $\Pi_{\mu\nu}$ is the photon self-energy. The asymptotic behavior of the potential is

$$V(R \to \infty) \sim \frac{e^{-m_{\rm el} R}}{R} \,. \tag{12}$$

We observe that the potential at large distances is not a Coulomb potential $(1/r)$ but a Yukawa potential $(e^{-\alpha r}/r)$, so that it goes to zero very rapidly at distances larger that $1/m_{\rm el}$. That is why $m_{\rm el}$ is called *screening mass*. The asymptotic behavior of the Fourier transform in (11) is determined by the singularity of the integrand closest to the origin, which in this case is a pole in the propagator $1/(k^2 + \Pi_{00}(0,\mathbf{k}))$; therefore, the electric screening mass satisfies [23]:

$$k^2 \; + \; \Pi_{00}(0,\mathbf{k}) \; = \; 0 \qquad \text{at } k^2 = -m_{\rm el}^2 \,. \tag{13}$$

Analogously, the screening mass m_s for the Φ^4 theory is given by the location of the pole of the static ($\omega = 0$) propagator:

$$k^2 \; + \; \Pi(0,\mathbf{k}) \; = \; 0 \qquad \text{at } k^2 = -m_{\rm s}^2 \,, \tag{14}$$

where $\Pi(\omega,\mathbf{k})$ is the self-energy of Φ.

The effective lagrangian has to be compatible with the symmetries of the original theory; *i.e.*, it has to be symmetric under the exchange $\phi \to -\phi$. Then, the most general lagrangian is of the form

$$\mathcal{L}_{\rm eff} = \frac{1}{2} \, (\boldsymbol{\nabla}\phi)^2 \; + \; \frac{1}{2} m^2 \, \phi^2 \; + \; \frac{1}{4!} \lambda \, \phi^4 \; + \; \frac{1}{6!} \lambda_6 \, \phi^6 \; + \; \delta\mathcal{L} \,, \tag{15}$$

where m^2, λ, and λ_6 are coupling constants of the effective theory. $\delta\mathcal{L}$ represents an infinite series of nonrenormalizable terms, each of them with a corresponding effective coupling constant. At leading order, any effective parameter will be proportional to T raised to the power required by dimensional analysis; the leading power of g^2 is determined by identifying the lowest order diagram that contributes to that parameter. The leading-order contributions to m^2, λ, and λ_6 are shown in Figs. 2 (a), (b), and (c), respectively. By counting the powers of the coupling constant in the diagrams and using dimensional analysis to determine the powers of T, their magnitudes must be

$$m^2 \sim g^2T^2\,, \tag{16}$$

$$\lambda \sim g^2T\,, \tag{17}$$

$$\lambda_6 \sim g^6\,. \tag{18}$$

If we are interested in calculations up to order g^4, we can drop the ϕ^6-term in $\mathcal{L}_{\rm eff}$, since it only contributes at higher order. Similarly, the non-renormalizable terms included in $\delta\mathcal{L}$ can also be neglected. What remains is a super-renormalizable effective theory.

The effective coupling λ is computed by matching the full theory and the effective theory. Let us consider the action of the full theory defined by the lagrangian (6)

$$S_{\rm full} = \int_0^{1/T} d\tau \int d^3x \,\left[\frac{1}{2}(\partial\Phi)^2 + \frac{g^2}{4!}\Phi^4\right], \tag{19}$$

Now, we use the expansion of Φ in terms of its Fourier modes (4),

$$\Phi(\mathbf{x},\tau) = T\sum_n \phi_n(\mathbf{x})e^{i\omega_n\tau}\,, \tag{20}$$

and write $S_{\rm full}$ as the sum of two terms; the first of them only depends on the static mode of the field and the second term also depends on the nonstatic modes. After integrating over τ, we get

$$S_{\rm full} = \int d^3x \,\left[\frac{1}{2}T(\nabla\phi_0)^2 + \frac{1}{4!}g^2T^3\phi_0^4\right] + \widetilde{S}_{\rm full}[\phi_0,\phi_n]\,. \tag{21}$$

Since the first term does not depend on the nonstatic modes, it does not change after integrating over the nonstatic modes. As a consequence it can be compared directly with the action of the effective theory. After rescaling $\phi \to \sqrt{T}\phi_0$ in the effective lagrangian (15) so that the kinetic terms match, we obtain

$$S_{\rm eff} = \int d^3x \,\left[\frac{1}{2}T(\nabla\phi_0)^2 + \frac{1}{4!}\lambda T^2\phi_0^4\right]. \tag{22}$$

Comparing (21) and (22), we conclude that

$$\lambda = g^2T \tag{23}$$

We have ignored the integration of $\widetilde{S}_{\rm full}$ over the nonstatic fields ϕ_n because we only want to obtain λ at leading order. This integration contributes to λ starting at next-to-leading-order and generates the contributions to the other parameters of the effective lagrangian (15) such as m^2, λ_6, etc.

The actual evaluation of the effective parameters is, in general, performed by matching the full and effective theories in the region where they describe the same physics. This region corresponds to large distances $R \gg 1/T$; therefore, we have to match physical quantities whose Feynman diagrams have a typical external momentum much smaller than T ($p_{\rm ext} \ll T$). In particular, m^2 is determined by matching the electric screening mass m_s. In the effective theory, the screening mass is defined by

$$k^2 \,+\, m^2 \,+\, \Pi_{\rm eff}(\mathbf{k}) \,=\, 0 \qquad \text{at } k^2 = -m_{\rm s}^2\,, \tag{24}$$

where $\Pi_{\rm eff}(\mathbf{k})$ is the self-energy of ϕ. We could compute m_s in both the full theory and the effective theory and then match them to determine m^2. In the full theory we would have to resum infinite series of diagrams such as those described at the beginning of Sect. 2.

There is an alternative method that greatly reduces the effort required to determine the parameters in the effective theory. It involves introducing an infrared cutoff Λ_{IR} satisfying $gT \ll \Lambda_{IR} \ll T$ on the internal momenta $p_{\rm int}$ of diagrams contributing to the physical quantity that we want to compute. In the full theory the infrared cutoff should satisfy $gT \ll \Lambda_{IR} \ll T$ and in the effective theory $m \ll \Lambda_{IR} \ll \Lambda$, where Λ is the ultraviolet cutoff of the effective theory. In the full theory with an infrared cutoff $p_{\rm int} > \Lambda_{IR}$, there are no complications from infrared divergences since $\Lambda_{IR} \gg gT$. We can therefore avoid resummations and compute using the *strict perturbation expansion* in powers of g^2. In the effective theory, with an infrared cutoff $p_{\rm int} > \Lambda_{IR}$, calculations can also be simplified. Since the leading order contribution to m^2 is of order g^2T^2 and $\Lambda_{IR} \gg gT$, we can treat m^2 as a perturbation and take the propagator of ϕ to be simply $1/k^2$. In what follows I will refer to the resulting perturbative expansion as the *strict perturbation expansion* of the effective theory. By construction, our effective theory is equivalent to the full theory at low momentum. Therefore, the infrared cutoff modifies the full theory and the effective theory in precisely the same way. We can therefore match the strict perturbation expansions of the full and effective theories to extract the effective parameters.

Note that we use the strict perturbation expansion only as a device to determine the effective parameters. To actually calculate physical quantities we must remove the infrared cutoff. In the effective theory, this will require using $1/(k^2 + m^2)$ as the propagator of the field ϕ instead of $1/k^2$.

Although we have used a momentum cutoff for illustration, we can determine the effective parameters by matching the strict perturbation expansions of the full and effective theories with any infrared regulator. As we will see, a particularly convenient choice for the infrared cutoff is dimensional regularization. While this method does not explicitly cut off the low momentum region from internal loops, it still allows the consistent calculation of a strict perturbation expansion for both the full theory and the effective theory.

We now proceed to calculate the mass parameter m^2 in the effective lagrangian (15) for the Φ^4 theory by matching calculations of the screening mass defined by (14) in the full theory and by (24) in the effective theory. The diagrams in the full theory that contribute to $\Pi(0, \mathbf{k})$ are the ones shown in Fig. 3. Now, if the g^{2n}-order contribution to $\Pi(k^2)$ is called $\Pi^{(n)}(k^2)$, the definition (14) tells us that:

$$m_{\rm s}^2 = \Pi(k^2 = -m_{\rm s}^2) = \Pi^{(1)}(-m_{\rm s}^2) + \Pi^{(2)}(-m_{\rm s}^2) + \cdots\,. \tag{25}$$

The first term $\Pi^{(1)}(-m_{\rm s}^2)$ is given explicitly in (7). It is independent of its argument and of order g^2T^2. Therefore, at leading order $m_s \sim g^2T^2$. Since the argument of $\Pi^{(n)}(-m_s^2)$ is of order g^2T^2, the strict perturbation expansion for the right side of (25) is obtained by making a Taylor expansion around 0. $\Pi^{(2)}(-m_s^2)$ is already of order g^4, we can set its argument to zero up to corrections of order g^4. We conclude that

$$m_{\rm s}^2 \approx \frac{Z_g^2 g^2}{2} \not\!\!\sum_P \frac{1}{P^2} \;-\; \frac{g^4}{4} \not\!\!\sum_P \frac{1}{P^2} \not\!\!\sum_P \frac{1}{(P^2)^2} \;-\; \frac{g^4}{6} \not\!\!\sum_{PQ} \frac{1}{P^2Q^2(P+Q)^2}\,. \tag{26}$$

Here and below, the symbol "$\approx$" denotes an equality that holds only in the strict perturbation expansion. To the order required, renormalization of the coupling constant in the $\overline{\rm MS}$ scheme is accomplished by the substitution

$$Z_g \;=\; 1 \;+\; \frac{3}{4\epsilon}\left(\frac{g}{4\pi}\right)^2\,. \tag{27}$$

The integrals in (26) are evaluated in Ref. [9] and the final result is

$$m_s^2 \approx \frac{1}{24}g^2T^2\left\{1+\left[\frac{1}{\epsilon}+\log\frac{\Lambda}{4\pi T}+2-\gamma+2\frac{\zeta'(-1)}{\zeta(-1)}\right]\left(\frac{g}{4\pi}\right)^2\right\}\,, \tag{28}$$

where Λ is the mass scale introduced by dimensional regularization.

The diagrams in the effective theory that contribute to $\Pi_{\rm eff}(\mathbf{k})$ are shown in Fig. 3 (where, the propagators and vertices are now those of the effective theory) and in Fig. 4. After expanding around $k^2 = 0$, there is no mass scale in the integrals and the loop diagrams vanish in dimensional regularization,

$$\Pi_{\rm eff}(0) = \delta m^2\,. \tag{29}$$

Consequently, from the definition (24),

$$m_{\rm s}^2 \approx m^2 + \delta m^2\,. \tag{30}$$

We obtain m^2 by matching (28) and (30). δm^2 in (30) is the mass counterterm that contains the poles in ϵ that are associated with the mass renormalization. Therefore, it is determined to be

$$\delta m^2 = \frac{1}{24}g^2T^2\left(\frac{g}{4\pi}\right)^2\frac{1}{\epsilon} \tag{31}$$

The Λ-dependence from the logarithm in (26) is partially cancelled by the Λ-dependence of the running coupling constant. The renormalization group equation for the coupling constant,

$$\mu\frac{d}{d\mu}\left(\frac{g}{4\pi}\right)^2 = 3\left(\frac{g}{4\pi}\right)^4\,, \tag{32}$$

gives

$$g^2(\Lambda) = g^2(\mu)\left[1-3\left(\frac{g}{4\pi}\right)^2\log\frac{\mu}{\Lambda}\right]\,, \tag{33}$$

which can be used to shift the renormalization scale Λ to an arbitrary scale μ. We conclude

$$m^2(\Lambda) = \frac{1}{24} g^2(\mu) T^2 \left\{ 1 + \left[-3 \log \frac{\mu}{4\pi T} + 4 \log \frac{\Lambda}{4\pi T} + 2 - \gamma + 2 \frac{\zeta'(-1)}{\zeta(-1)} \right] \left(\frac{g}{4\pi} \right)^2 \right\} . \quad (34)$$

Note that $m^2(\Lambda)$ depends logarithmically on the ultraviolet cutoff Λ at order g^4; this dependence is necessary to cancel logarithmic ultraviolet divergences from loop integrals in the effective theory. One should not confuse this ultraviolet cutoff Λ of the effective theory with the infrared cutoff Λ_{IR}. The latter is removed in the matching process. We can explicitly see this while using dimensional regularization by introducing two different regularization scales Λ and Λ_{IR} to regularize the ultraviolet and infrared divergences respectively. The scale Λ in (28) should be identified with the infrared scale Λ_{IR}. The expression (30) for the screening mass in the effective theory is then modified to

$$m_s^2 \approx m^2(\Lambda) + \frac{1}{24} g^2 T^2 \left[\frac{1}{\epsilon} - \left(\frac{g}{4\pi} \right)^2 \log \frac{\Lambda}{\Lambda_{IR}} \right] . \quad (35)$$

Matching both results the dependence on Λ_{IR} cancels and we recover (34) for $m^2(\Lambda)$.

Now, having determined m^2, we can use the effective theory to compute the screening mass. Remember that now, the ϕ field propagator is $1/(k^2+m^2)$, instead of $1/k^2$. Considering (24), $\Pi_{\rm eff}$ is given by the diagrams shown in Figs. 3 and 4 evaluated at the point $k = im$. We obtain [9]

$$m_s^2 \;=\; m^2(\Lambda) \left\{ 1 \;-\; 2\, \frac{\lambda}{16\pi m} \;-\; \frac{2}{3} \left[4 \log \frac{\Lambda}{2m} + 3 - 8 \log 2 \right] \left(\frac{\lambda}{16\pi m} \right)^2 \right\}. \quad (36)$$

Now, we can compute the screening mass by inserting (34) and (23) in (36). We find

$$\begin{aligned} m_s^2 \;&=\; \frac{1}{24}\, g^2 (2\pi T)\, T^2 \left\{ 1 - \sqrt{6}\, \frac{g}{4\pi} \right. \\ &+ \left. \left[4 \log \frac{g}{4\pi\sqrt{6}} - 1 + 11 \log 2 - \gamma + 2 \frac{\zeta'(-1)}{\zeta(-1)} \right] \left(\frac{g}{4\pi} \right)^2 \right\}, \end{aligned} \quad (37)$$

where we have set $\mu = 2\pi T$. Note that the dependence of m^2 on Λ in (34) has been cancelled by the ultraviolet cutoff introduced to regularize the effective theory. The term of order g^3 in (37) was first computed by Dolan and Jackiw [22]. The correction of order g^4 was obtained by Braaten and Nieto [9].

It is worth stressing the distinction between m_s and $m(\Lambda)$. The screening mass contains contributions from both the scales T and gT. In the full theory, it may be obtained by resumming the infrared divergent diagrams containing self-energy insertions. On the other hand, $m(\Lambda)$ only contains contributions from the scale T. By matching (26) and (30) we see that it can be obtained by evaluating the screening mass in the full theory by using the strict perturbation expansion. We can therefore think of it as the contribution to m_s from the scale T.

The technique we have just applied to a massless scalar field with Φ^4 self-interaction remains essentially unchanged when applied to QCD. In the following sections, we will see how it is applied to computing the free energy of QCD.

3 Separation of Scales in QCD

The partition function of QCD is

$$\mathcal{Z} = \int \mathcal{D}A_\mu(\mathbf{x},\tau)\mathcal{D}q\mathcal{D}\overline{q}\exp\left\{-\int_0^\beta d\tau\int d\mathbf{x}\,\mathcal{L}_{\rm QCD}\right\}, \tag{38}$$

where the lagrangian is

$$\mathcal{L}_{\rm QCD} = \frac{1}{4}G^a_{\mu\nu}G^a_{\mu\nu} + \overline{q}\gamma_\mu D_\mu q\,, \tag{39}$$

$G^a_{\mu\nu} = \partial_\mu A^a_\nu - \partial_\nu A^a_\mu + g f^{abc}A^b_\mu A^c_\nu$ is the field strength, and g is the gauge coupling constant. All the quark fields have been assembled into the multi-component spinor q, and the gauge-covariant derivative acting on this spinor is $D_\mu = \partial_\mu + igA^a_\mu T^a$. Quarks are considered to be massless; therefore, our description is accurate provided that T is much greater than the masses of the quarks considered (m_q). Corrections from the nonzero quark masses are suppressed by powers of m_q/T. Quarks with masses M_q much greater than T can also be neglected as they give corrections suppressed by powers of T/M_q.

We will express our calculations in terms of the group-theory factors C_A, C_F, and T_F defined by

$$f^{abc}f^{abd} = C_A\delta^{cd}\,, \tag{40}$$

$$(T^aT^a)_{ij} = C_F\delta_{ij}\,, \tag{41}$$

$$\mathrm{tr}\left(T^aT^b\right) = T_F\delta^{ab}\,. \tag{42}$$

For an $SU(N_c)$ gauge theory with n_f quarks in the fundamental representation with masses much smaller that T, these factors are $C_A = N_c$, $C_F = (N_c^2-1)/(2N_c)$, and $T_F = n_f/2$. The dimensions of the adjoint representation and the fermion representation are $d_A = N_c^2 - 1$ and $d_F = N_c n_f$, respectively.

Now we consider the effective theory that results from integrating out the nonstatic modes, which is called Electrostatic QCD (EQCD). Such a theory is only made out of the static bosonic modes. The free energy density of QCD, $F = -T\log\mathcal{Z}/V$ can be expressed in terms of the effective theory as

$$F = T\left(f_E - \frac{\log\mathcal{Z}_{\rm EQCD}}{V}\right), \tag{43}$$

where

$$\mathcal{Z}_{\rm EQCD} = \int \mathcal{D}A_0(\mathbf{x})\mathcal{D}A_i(\mathbf{x})\exp\left\{-\int d\mathbf{x}\,\mathcal{L}_{\rm EQCD}\right\}. \tag{44}$$

and f_E is the coefficient of the unit operator that is omitted from the lagrangian. One can interpret $f_E T$ as the contribution to the free energy from the scale T.

The lagrangian is

$$\mathcal{L}_{\rm EQCD} = \frac{1}{4}G^a_{ij}G^a_{ij} + \frac{1}{2}(D_iA^a_0)(D_iA^a_0) + \frac{1}{2}m_E^2A^a_0A^a_0 + \frac{1}{8}\lambda_E(A^a_0A^a_0)^2 + \delta\mathcal{L}_{\rm EQCD}\,, \tag{45}$$

where $G^a_{ij} = \partial_iA^a_j - \partial_jA^a_i + g_E f^{abc}A^b_iA^c_j$ is the magnetostatic field strength with effective gauge coupling constant g_E. $\delta\mathcal{L}_{\rm EQCD}$ represents an infinite series of non-renormalizable terms. Note

that the effective field theory does not have an effective quark field because fermionic modes are integrated out completely; all the effects of the fermions are incorporated into the effective parameters.

Figures 5(a), (b), (c), and (d) show diagrams that contribute at leading order to the parameters of EQCD: f_E, m_E^2, g_E^2, and λ_E respectively. Counting the powers of g in the diagrams and using dimensional analysis to determine the powers of T, we find that the magnitudes of the parameters are

$$f_E \sim T^3 \tag{46}$$
$$m_E^2 \sim g^2T^2 \tag{47}$$
$$g_E^2 \sim g^2T \tag{48}$$
$$\lambda_E \sim g^4T\,. \tag{49}$$

The electrostatic field A_0 has a mass of order gT while the magnetostatic fields remain massless. Therefore, we can go further in separating the different scales of QCD at high temperature by integrating out A_0. We obtain an effective theory of EQCD which is called magnetostatic QCD (MQCD). The free energy density of QCD can be written

$$F = T\left(f_E + f_M - \frac{\log \mathcal{Z}_{\rm MQCD}}{V}\right)\,, \tag{50}$$

where

$$\mathcal{Z}_{\rm MQCD} = \int \mathcal{D}A_i(\mathbf{x}) \exp\left\{-\int d\mathbf{x}\,\mathcal{L}_{\rm MQCD}\right\}\,. \tag{51}$$

and

$$\mathcal{L}_{\rm MQCD} = \frac{1}{4}G_{ij}^aG_{ij}^a + \delta\mathcal{L}_{\rm MQCD}\,. \tag{52}$$

The lagrangian is only made out of magnetostatic fields with gauge coupling constant g_M; $\delta\mathcal{L}_{\rm MQCD}$ represents an infinite series of non-renormalizable terms.

Similarly as we did in the case of EQCD, we can identify the order of the leading contribution to the MQCD parameters. Figures 6 (a) and (b) show diagrams in EQCD that contribute at leading order to f_M and g_M^2 respectively. Counting the powers of g_E in the diagrams and using dimensional analysis to determine the powers of m_E, we find

$$f_M \sim m_E^3 \sim g^3T^3 \tag{53}$$
$$g_M^2 \sim g_E^2 \sim g^2T\,. \tag{54}$$

We can also see the order at which λ_E contributes by identifying its leading contribution to f_M; it is shown in Figure 6 (c) and turns out to be of order $\lambda_E m_E^2 \sim g^6T^3$. We see that it contributes to the free energy at order g^6; thus, if we are interested in the free energy at lower order, we can ignore λ_E. Similarly the non-renormalizable terms of EQCD can also be omitted.

The free energy of QCD can be written as

$$F = T\left[f_E(T,g;\Lambda_E) + f_M(m_E^2,g_E,\lambda_E,\ldots;\Lambda_E,\Lambda_M) + f_G(g_M,\ldots;\Lambda_M)\right]\,, \tag{55}$$

where we have defined

$$f_G \equiv -\frac{\log \mathcal{Z}_{\rm MQCD}}{V}\,. \tag{56}$$

The factorization scales Λ_E and Λ_M separate the scales T, gT, and g^2T. F is written as the sum of three terms each of them depending only on the parameters of the corresponding theory; their divergences are regulated by the factorization scale parameters.

We have already seen that the leading contributions to f_E and f_M are of order T^3 and $m_E^3 \sim g^3T^3$ respectively. The leading contribution to f_G can be obtaining by realizing that the only parameter with dimensions involved in MQCD is g_M and consequently the leading contribution is of order $g_M^6 \sim g^6T^3$. Since we are interested in computing the free energy of QCD up to order g^5 we can ignore the contribution from f_G; then, f_E and f_M are all that we need. We conclude that the free energy of QCD up to order g^5 is given by

$$F = T\left[f_E(T,g;\Lambda_E) + f_M(m_E^2, g_E;\Lambda_E)\right]\,. \tag{57}$$

Therefore, we have to determine f_E, m_E^2, and g_E by matching full QCD and EQCD and then calculate f_M using EQCD.

4 The parameters of EQCD

In this section we will compute the parameters that define EQCD: f_E, m_E^2, and g_E. They are all computed up to the order required to reach our goal of evaluating the free energy of QCD at order g^5.

4.1 Evaluation of g_E^2

In this section, we will compute g_E explicitly by comparing the actions of QCD and EQCD. To simplify the notation we only consider the Yang-Mills part of the lagrangian (39); then, the action of pure QCD is

$$S_{\rm QCD} = \frac{1}{4}\int_0^{1/T} d\tau \int d^3x\; G^a_{\mu\nu}G^a_{\mu\nu}\,, \tag{58}$$

where $G^a_{\mu\nu} = \partial_\mu A^a_\nu - \partial_\nu A^a_\mu + g f^{abc} A^b_\mu A^c_\nu$. Now, we use the expansion of A^a_μ in terms of its Fourier modes,

$$A^a_\mu(\mathbf{x},\tau) = T\sum_n (A^a_\mu)_n(\mathbf{x})\; e^{i\omega_n\tau}\,, \tag{59}$$

and write $S_{\rm QCD}$ as the sum of two terms; the first of them only depends on the static modes of the fields and the second on the nonstatic modes. After integrating over τ and rescaling $(A^b_i)_0 \to (A^b_i)_0/gT$, we get

$$S_{\rm QCD} = \frac{1}{4g^2T}\int d^3x\; G^a_{ij}G^a_{ij} + \widetilde{S}_{\rm QCD}[A_0, A_n]\,, \tag{60}$$

where $G^a_{ij} = \partial_i(A^a_j)_0 - \partial_j(A^a_i)_0 + f^{abc}(A^b_i)_0(A^c_j)_0$. Since the first term does not depend on the nonstatic modes, it does not change after integrating over the nonstatic modes. As a

consequence, it can be compared directly with the action of the effective theory obtained from the lagrangian (45). After the rescaling $A_i^a \to (A_i^a)_0/g_E$, the action for the effective theory is

$$S_{\rm EQCD} = \frac{1}{4g_E^2} \int d^3x \; G_{ij}^a G_{ij}^a \, . \tag{61}$$

Comparing (60) and (61), we conclude that

$$g_E^2 = g^2 T \, . \tag{62}$$

We have ignored the integration of $\widetilde{S}_{\rm QCD}$ over the nonstatic fields $(A_i^a)_n$ because we only want to obtain g_E at leading order. This integration contributes to g_E starting at next-to-leading-order and generates the contributions to the other parameters of the effective lagrangian (45) such as m_E^2, λ_E, etc.

4.2 Evaluation of m_E

The effective mass m_E is the contribution to the electric screening mass from the momentum scale of order T. In QCD, the electric screening mass $m_{\rm el}$ describes the asymptotic behavior of the potential between two color charges as in (12). The electric screening mass in QCD is sensitive to magnetostatic screening effects [3] and therefore requires a nonperturbative definition [15]. However, if one imposes an infrared cutoff that removes those magnetostatic effects [8], one can define a perturbative electric screening mass in terms of the location of the pole in the gluon propagator as in (13). Although the gluon self-energy is gauge dependent, the location of the pole of the propagator is gauge invariant [24]. Therefore, if we use a gauge-invariant infrared cutoff like dimensional regularization, then the perturbative electric screening mass is gauge-invariant.

In full QCD with an infrared cutoff, the perturbative electric screening mass $m_{\rm el}$ is the solution to the equation

$$k^2 \, + \, \Pi(k^2) \, = \, 0 \qquad \text{at } k^2 = -m_{\rm el}^2, \tag{63}$$

where $\Pi(k^2)$ is obtained from the $\mu = \nu = 0$ component of the gluon self-energy tensor evaluated at $k_0 = 0$: $\Pi_{00}^{ab}(k_0 = 0, \mathbf{k}) = \Pi(k^2)\delta^{ab}$. In EQCD with an infrared cutoff, the perturbative electric screening mass $m_{\rm el}$ gives the location of the pole in the propagator for the field $A_0^a(\mathbf{x})$. Denoting the self-energy function by $\Pi_E(k^2)\delta^{ab}$, $m_{\rm el}$ is the solution to

$$k^2 \, + \, m_E^2 \, + \, \Pi_E(k^2) \, = \, 0 \qquad \text{at } k^2 = -m_{\rm el}^2. \tag{64}$$

By matching the expressions for $m_{\rm el}$ obtained by solving (63) and (64), we can determine the parameter m_E^2.

We calculate the perturbative electric mass $m_{\rm el}$ in the full theory using a strict perturbation expansion in g^2 and using dimensional regularization with $3 - 2\epsilon$ spatial dimensions to cut off both infrared and ultraviolet divergences. Expanding the function $\Pi^{(1)}(-m_s^2)$ on the right side of (25) in powers of m_s^2 and using the fact that the solution at lowest order is $m_s^2 = \Pi^{(1)}(0)$, the resulting expression for the perturbative electric screening mass to next-to-leading order in g^2 is

$$m_{\rm el}^2 \, \approx \, \Pi^{(1)}(0) \, - \, \Pi^{(1)}(0) \frac{d\Pi^{(1)}}{dk^2}(0) \, + \, \Pi^{(2)}(0) \, . \tag{65}$$

The one-loop diagrams that contribute to $\Pi^{(1)}(k^2)$ are shown in Fig. 7 and two-loop diagrams that contribute to $\Pi^{(1)}(k^2)$ are shown in Fig. 8; their analytical evaluation is detailed in [11]. We find that the strict perturbation expansion for $m_{\rm el}^2$ to order g^4 is

$$\begin{aligned} m_{\rm el}^2 \;\approx\; & \frac{1}{3}g^2(\Lambda)T^2\Bigg\{C_A + T_F \\ & + \epsilon\left[C_A\left(2\frac{\zeta'(-1)}{\zeta(-1)} + 2\log\frac{\Lambda}{4\pi T}\right)\right. \\ & \left. + T_F\left(1 - 2\log 2 + 2\frac{\zeta'(-1)}{\zeta(-1)} + 2\log\frac{\Lambda}{4\pi T}\right)\right] \\ & + \left[C_A^2\left(\frac{5}{3} + \frac{22}{3}\gamma + \frac{22}{3}\log\frac{\Lambda}{4\pi T}\right)\right. \\ & + C_A T_F\left(3 - \frac{16}{3}\log 2 + \frac{14}{3}\gamma + \frac{14}{3}\log\frac{\Lambda}{4\pi T}\right) \\ & \left. + T_F^2\left(\frac{4}{3} - \frac{16}{3}\log 2 - \frac{8}{3}\gamma - \frac{8}{3}\log\frac{\Lambda}{4\pi T}\right) \;-\; 6C_F T_F\right]\left(\frac{g}{4\pi}\right)^2\Bigg\}\,. \end{aligned} \tag{66}$$

In the order g^2 term, we have kept terms of order ϵ for later use.

The expression (66) for $m_{\rm el}^2$ is an expansion in powers of g^2. It does not include a g^3 term, in contrast to the expression for $m_{\rm el}^2$ that correctly incorporates the effects of the screening of electrostatic gluons [23]. This g^3 term arises because the g^4 correction includes a linear infrared divergence that is cut off at the scale gT. Since we have used dimensional regularization as an infrared cutoff, power infrared divergences such as this linear divergence have been set equal to zero.

In order to match with the expression (66), we have to calculate the perturbative electric screening mass $m_{\rm el}$ in EQCD using the strict expansion in g^2. Since m_E^2 is treated as a perturbation parameter of order g^2, the only scale in the self-energy function $\Pi_E(k^2)$ is k^2. After Taylor expanding in powers of k^2, there is no scale in the dimensionally regularized integrals; therefore, they all vanish. The solution to the equation (64) for the perturbative electric screening mass is therefore trivial:

$$m_{\rm el}^2 \;\approx\; m_E^2. \tag{67}$$

Now, we compare (66) and (67) and take the limit $\epsilon \to 0$. Note that the expression (66) depends on Λ explicitly through logarithms of $\Lambda/4\pi T$ and implicitly through the coupling constant $g^2(\Lambda)$. We shift the scale of the coupling constant from Λ to an arbitrary scale μ by using the renormalization group equation for the running coupling constant

$$g^2(\Lambda) \;=\; g^2(\mu)\left[1 \;+\; \frac{2(11C_A - 4T_F)}{3}\left(\frac{g}{4\pi}\right)^2\log\frac{\mu}{\Lambda}\right]. \tag{68}$$

After making this shift in the scale of the coupling constant, the remaining Λ can be identified with the factorization scale Λ_E that separates the scales T and gT. We conclude that the parameter m_E^2 is given by

$$m_E^2 \;=\; \frac{1}{3}\,g^2(\mu)\,T^2\Bigg\{C_A + T_F$$

$$
\begin{aligned}
&+ \left[C_A^2\left(\frac{5}{3}+\frac{22}{3}\gamma+\frac{22}{3}\log\frac{\mu}{4\pi T}\right)\right. \\
&+ C_A T_F\left(3-\frac{16}{3}\log 2+\frac{14}{3}\gamma+\frac{14}{3}\log\frac{\mu}{4\pi T}\right) \\
&\left.+ T_F^2\left(\frac{4}{3}-\frac{16}{3}\log 2-\frac{8}{3}\gamma-\frac{8}{3}\log\frac{\mu}{4\pi T}\right) - 6C_F T_F\right]\left(\frac{g}{4\pi}\right)^2\Bigg\}. \qquad (69)
\end{aligned}
$$

At this order in g^2, there is no dependence on the factorization scale Λ_E.

4.3 Evaluation of f_E

In this subsection, we calculate the coefficient of the unit operator f_E to next-to-next-to-leading order in g^2. The physical interpretation of f_E is that $f_E T$ is the contribution to the free energy from large momenta of order T. The parameter f_E is determined by calculating the free energy as a strict perturbation in g^2 in both full QCD and EQCD, and matching the two results.

In the full theory, the free energy has a diagrammatic expansion that begins with the one-loop, two-loop and three-loop diagrams shown in Figs. 9, 10, and 11. Evaluating these diagrams in Feynman gauge, we obtain after renormalization of the coupling constant (details can be found in [11])

$$
\begin{aligned}
F \;\approx\; & -\frac{\pi^2 d_A}{9}T^4\Bigg\{\frac{1}{5}+\frac{7}{20}\frac{d_f}{d_A}-\left(C_A+\frac{5}{2}T_F\right)\left(\frac{g}{4\pi}\right)^2 \\
&+\left[C_A^2\left(\frac{12}{\epsilon}+\frac{194}{3}\log\frac{\Lambda}{4\pi T}+\frac{116}{5}+4\gamma+\frac{220}{3}\frac{\zeta'(-1)}{\zeta(-1)}-\frac{38}{3}\frac{\zeta'(-3)}{\zeta(-3)}\right)\right. \\
&+C_A T_F\left(\frac{12}{\epsilon}+\frac{169}{3}\log\frac{\Lambda}{4\pi T}\right. \\
&\qquad\left.+\frac{1121}{60}-\frac{157}{5}\log 2+8\gamma+\frac{146}{3}\frac{\zeta'(-1)}{\zeta(-1)}-\frac{1}{3}\frac{\zeta'(-3)}{\zeta(-3)}\right) \\
&+T_F^2\left(\frac{20}{3}\log\frac{\Lambda}{4\pi T}+\frac{1}{3}-\frac{88}{5}\log 2+4\gamma+\frac{16}{3}\frac{\zeta'(-1)}{\zeta(-1)}-\frac{8}{3}\frac{\zeta'(-3)}{\zeta(-3)}\right) \\
&\left.+C_F T_F\left(\frac{105}{4}-24\log 2\right)\right]\left(\frac{g}{4\pi}\right)^4\Bigg\}, \qquad (70)
\end{aligned}
$$

where $g = g(\Lambda)$. The symbol "$\approx$" is a reminder of the strict perturbation expansion of the full theory.

In EQCD, the free energy is given by the expression (43). We calculate $\log \mathcal{Z}_{\rm EQCD}$ using the strict perturbation expansion in which g_E^2 and m_E^2 are treated as perturbation parameters and both infrared and ultraviolet divergences are regularized using dimensional regularization. Since diagrams with massless propagators and with no external legs vanish in dimensional regularization, the only contribution to $\log \mathcal{Z}_{\rm EQCD}$ which does not vanish comes from the counterterm δf_E which cancels ultraviolet divergences proportional to the unit operator. The resulting expression for the free energy is simply

$$
F \;\approx\; (f_E + \delta f_E)\, T\,. \qquad (71)
$$

The counterterm can be determined by calculating the ultraviolet divergences in $\log \mathcal{Z}_{\rm EQCD}$. If we use dimensional regularization together with a minimal subtraction renormalization scheme in the effective theory, then δf_E is a polynomial in g_E^2, m_E^2, and the other parameters in the lagrangian for EQCD. The only combination of parameters that has dimension 3 and is of order g^4 is $g_E^2 m_E^2$. Thus the leading term in δf_E is proportional to $g_E^2 m_E^2$. The coefficient is determined by a 2-loop calculation that is a trivial part of the 3-loop calculation in Section 5.1. The result for the counterterm is

$$\delta f_E \;=\; -\frac{d_A C_A}{4(4\pi)^2} g_E^2 m_E^2 \frac{1}{\epsilon} \,. \tag{72}$$

When expressing this counterterm in terms of the parameters g and T of the full theory, we must take into account the fact that m_E^2 multiplies a pole in ϵ. Thus in addition to expression for m_E^2 given in (69), we must also include the terms of order ϵ which can be extracted from (66). The counterterm (72) is therefore

$$\begin{aligned}\delta f_E \;=\; & -\frac{\pi^2 d_A}{9}\left(\frac{g}{4\pi}\right)^4 T^3 \;\left[12 C_A^2\left(\frac{1}{\epsilon}+2\frac{\zeta'(-1)}{\zeta(-1)}+2\log\frac{\Lambda_E}{4\pi T}\right)\right. \\ & \left. +\,12 C_A T_F\left(\frac{1}{\epsilon}+1-2\log 2+2\frac{\zeta'(-1)}{\zeta(-1)}+2\log\frac{\Lambda_E}{4\pi T}\right)\right] \,. \end{aligned} \tag{73}$$

Note that minimal subtraction in the effective theory is not equivalent to minimal subtraction in the full theory. In addition to the poles in ϵ in (73), there are finite terms that depend on the factorization scale Λ_E.

Matching (70) with (71) and using the expression (73), we conclude that f_E to order g^4 is

$$\begin{aligned} f_E(\Lambda_E) \;=\; & -\frac{\pi^2 d_A}{9} T^3 \Bigg\{ \left(\frac{1}{5}+\frac{7}{20}\frac{d_F}{d_A}\right) \;-\; \left(C_A+\frac{5}{2}T_F\right)\left(\frac{g}{4\pi}\right)^2 \\ & +\Bigg(C_A^2\left[48\log\frac{\Lambda_E}{4\pi T}-\frac{22}{3}\log\frac{\mu}{4\pi T}\right. \\ & \qquad \left. +\frac{116}{5}+4\gamma+\frac{148}{3}\frac{\zeta'(-1)}{\zeta(-1)}-\frac{38}{3}\frac{\zeta'(-3)}{\zeta(-3)}\right] \\ & +C_A T_F\left[48\log\frac{\Lambda_E}{4\pi T}-\frac{47}{3}\log\frac{\mu}{4\pi T}\right. \\ & \qquad \left. +\frac{401}{60}-\frac{37}{5}\log 2+8\gamma+\frac{74}{3}\frac{\zeta'(-1)}{\zeta(-1)}-\frac{1}{3}\frac{\zeta'(-3)}{\zeta(-3)}\right] \\ & +T_F^2\left[\frac{20}{3}\log\frac{\mu}{4\pi T}+\frac{1}{3}-\frac{88}{5}\log 2+4\gamma+\frac{16}{3}\frac{\zeta'(-1)}{\zeta(-1)}-\frac{8}{3}\frac{\zeta'(-3)}{\zeta(-3)}\right] \\ & +C_F T_F\left[\frac{105}{4}-24\log 2\right]\Bigg)\left(\frac{g}{4\pi}\right)^4\Bigg\} \,, \end{aligned} \tag{74}$$

where $g = g(\mu)$ is the coupling constant in the $\overline{\rm MS}$ renormalization scheme at the scale μ. We have used (68) to shift the scale of the running coupling constant from Λ to an arbitrary renormalization scale μ, and we have identified the explicit factors of Λ that remain with the factorization scale Λ_E.

5 The Free Energy of QCD

Once we have understood how to resolve the contributions of the various momentum scales in thermal QCD, asymptotic freedom guarantees us that perturbation theory will be under control in the high temperature limit. At sufficiently high temperature, the running coupling constant will be small enough that calculations to leading order in g will be accurate. However, in most practical applications, such as those encountered in heavy ion collisions, the temperature is not asymptotically large, and we must worry about higher order corrections. The accuracy of the perturbation expansion can only be assessed by carrying out explicit perturbative calculations beyond leading order. One of the obstacles to progress in high temperature field theory has been that the technology for perturbative calculations was not well developed. Only very recently have there been any calculations to a high enough order that the running of the coupling constant comes into play. The simplest physical observable that can be calculated in perturbation theory is the free energy, which determines all the static thermodynamic properties of the system. The running of the coupling constant first enters at order g^4. The free energy for gauge theories at zero temperature but large chemical potential was calculated to order g^4 long ago [25]. The first such calculation at high temperature was the free energy of a scalar field theory with a ϕ^4 interaction, which was calculated to order g^4 by Frenkel, Saa, and Taylor in 1992 [26]. (A technical error was later corrected by Arnold and Zhai [20].) The analogous calculations for gauge theories were carried out in 1994. The free energy for QED was calculated to order e^4 by Corianò and Parwani [27] and the free energy for a non-Abelian gauge theory was calculated to order g^4 by Arnold and Zhai [20]. The calculation of Arnold and Zhai was completely analytic, and thus represent a particularly significant leap in calculational technology. The calculational frontier has since been extended to fifth order in the coupling constant by Parwani and Singh [28] and by Braaten and Nieto [9] for ϕ^4 theory, by Parwani [29] and Andersen [14] for QED, and by Kastening and Zhai [30] and Braaten and Nieto [10, 11] for non-Abelian gauge theories. In the following subsection, the calculation of the free energy for a non-Abelian gauge theory to order g^5 based on Ref. [10, 11] is presented. Also, the calculations that are required to obtain the free energy to order g^6 are outlined.

5.1 QCD free energy: up to order g^5

In order to reach our goal of obtaining the free energy of QCD to order g^5, it remains to evaluate the coefficient of the unit operator of MQCD, f_M, which is the contribution of the scale gT to the free energy.

Through order g^5, f_M is proportional to the logarithm of the partition function for EQCD:

$$f_M \;=\; -\frac{\log \mathcal{Z}_{\rm EQCD}}{V} \;. \tag{75}$$

The lagrangian of EQCD that we are considering at this point is

$$\mathcal{L}_{\rm EQCD} = \frac{1}{4}G_{ij}^a G_{ij}^a + \frac{1}{2}(D_i A_0)^2 + \frac{1}{2}m_E^2 A_0^2 \;, \tag{76}$$

where now the parameters g_E and m_E are known. In order to calculate the contribution to f_M using perturbation theory, we must incorporate the terms in the lagrangian that provide

electrostatic screening into the free part of the lagrangian. The necessary screening effects are provided by the $A_0^a A_0^a$ term in the EQCD lagrangian. Thus we must include the effects of the mass parameter m_E^2 to all orders, while treating all the other coupling constants of EQCD as perturbation parameters. The only coupling constant that is required to obtain the free energy to order g^5 is the gauge coupling constant g_E.

The contributions to $\log \mathcal{Z}_{\rm EQCD}$ of orders g^3, g^4, and g^5 are given by the sum of the 1-loop, 2-loop, and 3-loop diagrams in Figs. 12, 13, and 14. The solid, wavy, dashed lines represent the propagators of the A_0 field, the A_i fields, and the associated ghosts, respectively. We evaluate these diagrams in Feynman gauge. The details of this calculation may be found in [11] where the methods developed by Broadhurst [31] were used to evaluate analytically the integrals involved by the 3-loop diagrams. The resulting expression for the logarithm of the partition function is

$$\begin{aligned} f_M \;=\; & -\frac{d_A}{3(4\pi)} m_E^3 \;+\; \frac{d_A C_A}{4(4\pi)^2}\left(\frac{1}{\epsilon} + 4\log\frac{\Lambda}{2m_E} + 3\right) g_E^2 m_E^2 \\ & + \frac{d_A C_A^2}{(4\pi)^3}\left(\frac{89}{24} - \frac{11}{6}\log 2 + \frac{1}{6}\pi^2\right) g_E^4 m_E \;+\; \delta f_E \;, \end{aligned} \tag{77}$$

where δf_E is the counterterm associated with the unit operator of the EQCD lagrangian and Λ is the scale of dimensional regularization. It can be identified with the ultraviolet cutoff Λ_E of EQCD. The ultraviolet pole in ϵ in the term proportional to $g_E^2 m_E^2$ in (77) is cancelled by the counterterm δf_E, which is given in (72). Our final result is therefore

$$\begin{aligned} f_M(\Lambda_E) \;=\; & -\frac{d_A}{3(4\pi)} m_E^3 \left\{ 1 \;+\; \left[-3\log\frac{\Lambda_E}{2m_E} - \frac{9}{4}\right]\frac{C_A g_E^2}{4\pi m_E} \right. \\ & \left. + \left[-\frac{89}{8} + \frac{11}{2}\log 2 - \frac{1}{2}\pi^2\right]\left(\frac{C_A g_E^2}{4\pi m_E}\right)^2 \right\}. \end{aligned} \tag{78}$$

The coefficient f_M in (78) can be expanded in powers of g by setting $g_E^2 = g^2 T$ and by substituting the expression (69) for m_E^2. The complete free energy to order g^5 is then $F = (f_E + f_M)T$. Note that the dependence on the arbitrary factorization scale Λ_E cancels between f_E and f_M, up to corrections that are higher order in g, leaving a logarithm of T/m_E. This $g^4 \log(g)$ term is associated with the renormalization of f_E, and its coefficient can be determined from the evolution equation [11]

$$\Lambda_E \frac{d}{d\Lambda_E} f_E \;=\; -\frac{d_A C_A}{(4\pi)^2} g_E^2 m_E^2 + O(g^6 T^3) \;. \tag{79}$$

There is no $g^5 \log(g)$ term in the perturbation expansion for F, and this is a consequence of the vanishing of the g_E^4 term in the evolution equation for m_E^2 analogous to (79).

5.2 QCD free energy: beyond order g^5

In 1980, Linde [32] pointed out a problem concerning perturbation theory at finite temperature. Let us consider diagrams that contribute to the free energy of QCD like the one in

Fig. 15 with $L+1$ loops. Its infrared behavior is described by an integral of the form

$$I = g^{2L} T^{L+1} \int \prod_{i=1}^{L+1} d^3k_i \prod_{j=1}^{2L} \frac{1}{k_j^2 + m^2}\,, \tag{80}$$

where we have inserted a mass m into the propagator as an infrared cutoff. From dimensional analysis we see that when

- $L < 3$, I is infrared finite.
- $L = 3$, $I \sim g^6 T^4 \log(T/m)$.
- $L > 3$, $I \sim g^6 T^4 (g^2 T/m)^{L-3}$.

This means that if we consider nonstatic gluons whose mass m is set by the Matsubara frequency which is of order T, then $I \sim g^6 T^4 (g^2)^{L-3}$; the magnitude of the contribution decreases by a factor g^2 for each loop as in ordinary perturbation theory. If we consider electrostatic gluons whose screening mass is of order gT, then $I \sim g^6 T^4 g^{L-3}$; the magnitude of the contribution decreases by a factor of g for each additional loop. However, if we consider magnetostatic gluons to be screened at a scale m of order g^2T, $I \sim g^6 T^4$; all of the diagrams contribute to order g^6, no matter how large the number of loops is.

This problem remained open for many years. In 1994, Braaten [7] proposed a solution of this puzzle in the context of the effective field theory approach we are reviewing here. Later, Braaten and Nieto [11] analyzed the diagrams that contribute to order g^6 from the different scales. The free energy is given by (55)

$$F = T(f_E + f_M + f_G)\,, \tag{81}$$

where f_E, f_M, and f_G give the contributions to the free energy from the scales T, gT, and g^2T respectively. We proceed to outline the calculations that would be required to obtain F to an accuracy of g^6. In the full theory, we have to calculate contributions to f_E from 4-loop diagrams and, also, the terms up to order g^4 and ϵg^4 for g_E^2 and λ_E. In EQCD, we need to calculate the 4-loop diagrams that give the term g_E^6 in f_M and the 1-loop diagram that gives the $\lambda_E m_E$ term. Also, g_E has to be computed up to order g^4. Finally, there is a contribution from MQCD which can be written in the form

$$f_G = \left(a + b \log \frac{\Lambda_M}{g_M^2}\right) g_M^6\,. \tag{82}$$

The number b may be calculated by evaluating the logarithmic ultraviolet divergence in 4-loop diagrams of MQCD, but the number a requires nonperturbative calculations. It can be calculated using lattice simulations of pure gauge theory in three dimensions. Recently, Karsch *et al.* [16] have reported lattice calculations that estimate the value of a.

The contributions to the free energy at higher order in g can be analyzed in a similar way. The contributions from the scales T and gT can all be obtained from diagrammatic calculations in full QCD and EQCD. The contributions from the scale g^2T require nonperturbative calculation in MQCD. It is clear that one can write an expansion for F in powers of g at arbitrary order. In this sense, there is no breakdown of the weak-coupling expansion at any order.

6 Convergence of Perturbation Theory

We have calculated the free energy as a perturbation expansion in powers of g to order g^5

$$F = (f_E + f_M)T \,, \tag{83}$$

where f_E is given by (74) and f_M by (78). In this section, we examine the convergence of that perturbation expansion; the analysis is based on Refs. [10, 11]. For simplicity, we focus on the case of QCD with n_f flavors of quarks. The expansion of the free energy in powers of $\sqrt{\alpha_s}$ with $\alpha_s = g^2/(4\pi)$ is

$$\begin{aligned} F \;=\; -\frac{8\pi^2}{45}T^4 \left[F_0 \;+\; F_2\frac{\alpha_s(\mu)}{\pi} \;+\; F_3\left(\frac{\alpha_s(\mu)}{\pi}\right)^{3/2} \;+\; F_4\left(\frac{\alpha_s}{\pi}\right)^2 \right. \\ \left. + F_5\left(\frac{\alpha_s}{\pi}\right)^{5/2} \;+\; O(\alpha_s^3 \log \alpha_s) \right] . \end{aligned} \tag{84}$$

The coefficients in this expansion are

$$F_0 \;=\; 1 + \tfrac{21}{32}n_f \,, \tag{85}$$

$$F_2 \;=\; -\frac{15}{4}\left(1 + \tfrac{5}{12}n_f\right) \,, \tag{86}$$

$$F_3 \;=\; 30\left(1 + \tfrac{1}{6}n_f\right)^{3/2} \,, \tag{87}$$

$$\begin{aligned} F_4 \;=\; & 237.2 + 15.97 n_f - 0.413 n_f^2 + \frac{135}{2}\left(1 + \tfrac{1}{6}n_f\right)\log\left[\frac{\alpha_s}{\pi}\left(1 + \tfrac{n_f}{6}\right)\right] \\ & - \frac{165}{8}\left(1 + \tfrac{5}{12}n_f\right)\left(1 - \tfrac{2}{33}n_f\right)\log\frac{\mu}{2\pi T} \,, \end{aligned} \tag{88}$$

$$\begin{aligned} F_5 \;=\; & \left(1 + \tfrac{1}{6}n_f\right)^{1/2}\left[-799.2 - 21.96 n_f - 1.926 n_f^2 \right. \\ & \left. + \frac{495}{2}\left(1 + \tfrac{1}{6}n_f\right)\left(1 - \tfrac{2}{33}n_f\right)\log\frac{\mu}{2\pi T}\right] . \end{aligned} \tag{89}$$

The coefficient F_2 was first given by Shuryak [33]. The coefficient of F_3 was calculated by Kapusta [34] and Kalashnikov and Klimov [35]. The coefficient of order $\alpha_s^2 \log \alpha_s$ was obtained by Toimela [36] and the coefficient of order α_s^2 by Arnold and Zhai [20]. The coefficient F_5 has also been calculated independently by Kastening and Zhai [30].

We now ask if the expansion (84) is well-behaved. If the series is apparently convergent, then it can plausibly be used to evaluate the free energy. We study the expression (84) at different temperatures $T > T_c \sim 200$ MeV. We choose the renormalization scale to be $\mu = 2\pi T$, which is the mass of the lightest nonstatic mode. In Table 1 we give the contributions coming from each order in $\sqrt{\alpha_s}$, rescaled so that the leading order term is 1. We see that the correction of order $\alpha_s^{5/2}$ is the largest unless the temperature T is greater than 2 GeV. The term of order $\alpha_s^{3/2}$ is smaller than the term of order α_s only when the temperature is greater than about 1 TeV.

T (GeV)	$\alpha_s(2\pi T)$	expansion for F
0.250	0.321	$1 - 0.282 + 0.583 + 0.276 - 1.094$
0.500	0.239	$1 - 0.210 + 0.374 + 0.010 - 0.524$
1	0.194	$1 - 0.167 + 0.267 + 0.033 - 0.287$
2	0.165	$1 - 0.142 + 0.209 + 0.011 - 0.191$
1000	0.074	$1 - 0.0624 + 0.0619 + 0.0106 - 0.0242$

Table 1: Perturbation expansion for the Free Energy F in units of $(-8\pi^2 T^4/45)F_0$ at different temperatures.

T (GeV)	$\alpha_s(2\pi T)$	expansion for f_E
0.250	0.321	$1 - 0.282 + 0.489$
0.500	0.239	$1 - 0.210 + 0.271$
1	0.194	$1 - 0.167 + 0.132$
2	0.165	$1 - 0.142 + 0.096$

Table 2: Perturbation expansion for f_E in units of $(-8\pi^2 T^4/45)F_0$ at different temperatures.

We can go further in our analysis provided that we have separated the contributions from the scales T and gT. We proceed to study the perturbation expansion at the scale T. The term f_E which gives the contribution to the free energy from the scale T is given in (74):

$$\begin{aligned} f_E(\Lambda_E) &= -\frac{8\pi^2}{45}T^3\Bigg\{1 + \tfrac{21}{32}n_f - \frac{15}{4}\left(1 + \tfrac{5}{12}n_f\right)\frac{\alpha_s(\mu)}{\pi} \\ &\quad + \Bigg[244.9 - 17.24n_f - 0.415n_f^2 \\ &\quad - \frac{165}{8}\left(1 + \tfrac{5}{12}n_f\right)\left(1 - \tfrac{2}{33}n_f\right)\log\frac{\mu}{2\pi T} \\ &\quad - 135\left(1 + \tfrac{1}{6}n_f\right)\log\frac{\Lambda_E}{2\pi T}\Bigg]\left(\frac{\alpha_s}{\pi}\right)^2 + O(\alpha_s^3)\Bigg\}. \end{aligned} \tag{90}$$

Again we choose the renormalization scale to be $\mu = 2\pi T$. We chose the factorization scale Λ_E to be $2\pi T$, to avoid large logarithms of $\Lambda_E/2\pi T$. Rescaling the contributions from each order in α_s, we obtain the expansion of f_E shown in Table 2. We see that the term of order α_s is reasonably small for all the values of T that are given. Note that one could choose Λ_E so that the contribution of order α_s^2 cancels. Therefore, the size of the order α_s^2 correction is not a very good test of the perturbation expansion.

It is interesting to study the convergence of the other parameter of EQCD that we have computed, m_E^2, which is given by (69):

$$m_E^2 = 4\pi\,\alpha_s(\mu)\,T^2\Bigg\{1 + \tfrac{1}{6}n_f + \Bigg[0.612 - 0.488n_f - 0.0428n_f^2$$

T (GeV)	$\alpha_s(2\pi T)$	expansion for m_E^2
0.250	0.321	$1 - 0.124$
0.500	0.239	$1 - 0.093$
1	0.194	$1 - 0.098$
2	0.165	$1 - 0.083$

Table 3: Perturbation expansion for m_E^2 in units of $4\pi\alpha_s(2\pi T)T^2(1 + n_f/6)$ at different temperatures.

T (GeV)	$\alpha_s(2\pi T)$	expansion for f_M
0.250	0.321	$1 - 1.050 - 1.694$
0.500	0.239	$1 - 1.047 - 1.262$
1	0.194	$1 - 0.947 - 0.930$
2	0.165	$1 - 0.935 - 0.791$

Table 4: Perturbation expansion for f_M in units of $-2/(3\pi)[4\pi\alpha_s(2\pi T)T^2(1 + n_f/6)]^{3/2}$ at different temperatures.

$$+ \frac{11}{2}\left(1+\tfrac{1}{6}n_f\right)\left(1-\tfrac{2}{33}n_f\right)\log\frac{\mu}{2\pi T}\Bigg]\frac{\alpha_s}{\pi} \;+\; O(\alpha_s^2)\Bigg\}\,. \tag{91}$$

Again, setting $\mu = 2\pi T$ we obtain the corrections to the leading order result that are summarized in Table 3. Here, we also see that the next-to-leading order correction is reasonably small for all the values of T. Based on these results, we conclude that the perturbation series for the parameters of EQCD are well-behaved even at temperatures as low as 250 MeV.

We next examine the behavior of the perturbation expansion for EQCD. The term f_M is given by (78):

$$\begin{aligned} f_M(\Lambda_E) \;&=\; -\frac{2}{3\pi}m_E^3\Bigg[1 \;-\; \left(0.256 + \frac{9}{2}\log\frac{\Lambda_E}{m_E}\right)\frac{g_E^2}{2\pi m_E} \\ &\qquad - 27.6\left(\frac{g_E^2}{2\pi m_E}\right)^2 \;+\; O(g^3)\Bigg]\,. \end{aligned} \tag{92}$$

We choose the renormalization scale of EQCD Λ_E to be m_E, which is mass of the electrostatic mode. In Table 4 we give the contribution at each order in g_E^2/m_E for the factor in square brackets in (92). The next-to-leading order correction could be made to vanish by a suitable choice of Λ_E. Therefore, it is not a good test of the convergence of the expansion. The next-to-next-to-leading order correction is independent of Λ_E and is smaller than the leading order term only if the temperature $T > 2$ GeV. Thus, the temperature for which the perturbation series for f_M is well-behaved is much higher than that required for the parameters of EQCD to have well-behaved perturbation series.

This analysis suggests that the slow convergence of the expansion for F in powers of $\sqrt{\alpha_s}$ may be attributed to the slow convergence of perturbation theory at the scale gT.

7 Conclusions

In this paper, we have reviewed effective-field-theory methods to study the high T limit of QCD. These methods have been used to unravel the contributions to the free energy of QCD at high temperature from the scales T, gT, and g^2T. Also, the free energy has been explicitly computed to order g^5 and the calculation of the g^6 contribution outlined. The calculation was significantly streamlined by using effective-field-theory methods to reduce every step of the calculation to one that involves only a single momentum scale.

Our explicit calculations allow us to study the convergence of the perturbation expansion for thermal QCD. They suggest that perturbation theory at the scale gT requires a much smaller value of the coupling constant than perturbation theory at the scale T. At the scale T, perturbative corrections are small for all temperatures $T > T_c \simeq 200$ MeV. Of course, even if this condition is satisfied, the perturbation expansion may break down anyway, but this is certainly a necessary condition. At the scale gT, perturbative corrections can be small only if $T > 2$ GeV. Thus, in order to achieve a given relative accuracy, the temperature T must be an order of magnitude larger for perturbation theory at the scale gT compared to perturbation theory at the scale T.

There is a range of temperatures in which perturbation theory at the scale gT has broken down, but perturbation theory at the scale T is reasonably accurate. In this case, one can still use perturbation theory at the scale T to calculate the parameters in the EQCD lagrangian. However, nonperturbative methods, such as lattice simulations of EQCD, are required to calculate the effects of the smaller momentum scales gT and g^2T. While one could simply treat the entire problem nonperturbatively using lattice simulations of full QCD, the effective-field-theory approach provides a dramatic savings in resources for numerical computation. The savings come from two sources. One is the reduction of the problem from a 4-dimensional field theory to a 3-dimensional field theory. The other source of savings is that quarks are integrated out of the theory, which reduces it to a purely bosonic problem.

Acknowledgements

This work was supported in part by the U. S. Department of Energy, Division of High Energy Physics, under Grant DE-FG02-91-ER40690. I would like to thank E. Braaten for many valuable discussions and reading the manuscript carefully.

References

[1] T. Appelquist and J. Carazzone, Phys. Rev. D **11**, 2856 (1975).

[2] T. Appelquist and R.D. Pisarski, Phys. Rev. D **23**, 2305 (1981).

[3] S. Nadkarni, Phys. Rev. D **27**, 917 (1983).

[4] D.J. Gross, R.D. Pisarski, and L.G. Yaffe, Rev. Mod. Phys. **53**, 43 (1981).

[5] H. Georgi, Annu. Rev. Nucl. Part. Sci. **43**, 209 (1993).

[6] A. Irbäck *et al.*, Nucl. Phys. **B363**, 34 (1991); T. Reisz, Z. Phys. C **53**, 169 (1992); L. Kärkkäinen *et al.*, Phys. Let. B **282**, 121 (1992); Nucl. Phys. **B395**, 733 (1993).

[7] E. Braaten, Phys. Rev. Lett. **74**, 2164 (1995).

[8] E. Braaten and A. Nieto, Phys. Rev. Lett. **74**, 3530 (1995).

[9] E. Braaten and A. Nieto, Phys. Rev. D **51**, 6990 (1995).

[10] E. Braaten and A. Nieto, Phys. Rev. Lett. **76**, 1417 (1996).

[11] E. Braaten and A. Nieto, Phys. Rev. D **53**, 3421 (1996).

[12] K. Farakos, K. Kajantie, K. Rummukainen, and M.E. Shaposhnikov, Phys. Lett. B **336**, 494 (1994); Nucl. Phys. **B425**, 67 (1994); **B442**, 317 (1995); K. Kajantie, M. Laine, K. Rummukainen, and M. Shaposhnikov, Nucl. Phys. **B458**, 90 (1996); **B466**, 189 (1996); Phys. Rev. Lett. **77**, 2887 (1996).

[13] M.E. Shaposhnikov, CERN-TH/96-280 (hep-ph/9610247).

[14] J.O. Andersen, Phys. Rev. D **53**, 7286 (1996); OSLO-TP-6-96 (hep-ph/9606357) to appear in Z. Phys. C.

[15] P. Arnold and L.G. Yaffe, Phys. Rev. D **52**, 7208 (1995).

[16] F. Karsch *et al.*, BI-TP-96-19 (hep-lat/9605031).

[17] J.M. Cline and K. Kainulainen, CERN-TH/96-76 (hep-ph/9605235); M. Losada, RU-96-25 (hep-ph/9605266); M. Laine, HD-THEP-96-13 (hep-ph/9605283).

[18] J. Kapusta, *Finite-Temperature Field Theory*, Cambridge University Press (1989).

[19] M. Le Bellac, *Thermal Field Theory*, Cambridge University Press (1996).

[20] P. Arnold and C. Zhai, Phys. Rev. D **50**, 7603 (1994); Phys. Rev. D **51**, 1906 (1995).

[21] N.P. Landsman, Nucl. Phys. **B322**, 498 (1989).

[22] L. Dolan and R. Jackiw, Phys. Rev. D **9**, 3320 (1974).

[23] A. Rebhan, Phys. Rev. D **48**, R3967 (1993); Nucl. Phys. **B340**, 319 (1994); E. Braaten and A. Nieto, Phys. Rev. Lett. **73**, 2402 (1994).

[24] R. Kobes, G. Kunstatter, and A. Rebhan, Phys. Rev. Lett. **64**, 2992 (1990); Nucl. Phys. **B355**, 1 (1991).

[25] B.A. Freedman and L.D. McLerran, Phys. Rev. D **16**, 1147 (1977); **16**, 1169 (1977); V. Baluni, Phys. Rev. D **17**, 2092 (1978).

[26] J. Frenkel, A.V. Saa, and J.C. Taylor, Phys. Rev. D **46**, 3670 (1992).

[27] C. Corianò and R.R. Parwani, Phys. Rev. Lett. **73**, 2398 (1994); R.R. Parwani and C. Corianò, Nucl. Phys. **B434**, 56 (1995).

[28] R. Parwani and H. Singh, Phys. Rev. D **51**, 4518 (1995).

[29] R.R. Parwani, Phys. Lett. **B334**, 420 (1994).

[30] B. Kastening and C. Zhai, Phys. Rev. D **52**, 7232 (1995).

[31] D.J. Broadhurst, Z. Phys. C **54**, 599 (1992).

[32] A.D. Linde, Rep. Prog. Phys. **42**, 389 (1979); Phys. Lett. **96B**, 289 (1980).

[33] E. Shuryak, J.E.T.P. **47**, 212 (1978).

[34] J.I. Kapusta, Nucl. Phys. **B148**, 461 (1979).

[35] O.K. Kalashnikov and V.V. Klimov, Sov. J. Nucl. Phys. **33**, 847 (1981).

[36] T.Toimela, Phys. Lett. **124B**, 407 (1983).

Figure Captions

1. Diagrams that contribute to the self-energy of ϕ^4.

2. Leading order contributions to the effective parameters of $\mathcal{L}_{\rm eff}$ for ϕ^4.

3. Diagrams that contribute to the self-energy up to 2-loop order for ϕ^4.

4. Diagrams that contribute to the self-energy up to 2-loop order for ϕ^4 involving the mass counterterm.

5. Leading order contributions to the parameters of EQCD: (a) f_E, (b) m_E^2, (c) g_E, and (d) λ_E.

6. Leading order contributions to the parameters of MQCD: (a) f_M, (b) g_M^2, and (c) the first contribution to f_M that involves λ_E. Solid and wavy lines represent the propagators of the A_0 field and the A_i fields, respectively. The solid blob represents the vertex associated with λ_E.

7. One-loop Feynman diagrams for the gluon self-energy. Curly lines, solid lines, and dashed lines represent the propagators of gluons, quarks, and ghosts, respectively.

8. Two-loop Feynman diagrams for the gluon self-energy. The solid blob represents the sum of the one-loop gluon self-energy diagrams shown in Fig. 7.

9. One-loop Feynman diagrams for the free energy of QCD.

10. Two-loop Feynman diagrams for the free energy of QCD.

11. Three-loop Feynman diagrams for the free energy of QCD.

12. One-loop Feynman diagram for the logarithm of the partition function of EQCD.

13. Two-loop Feynman diagram for the logarithm of the partition function of EQCD.

14. Three-loop Feynman diagrams for the logarithm of the partition function of EQCD.

15. Diagram that may give rise to the breakdown of perturbation theory in thermal QCD.

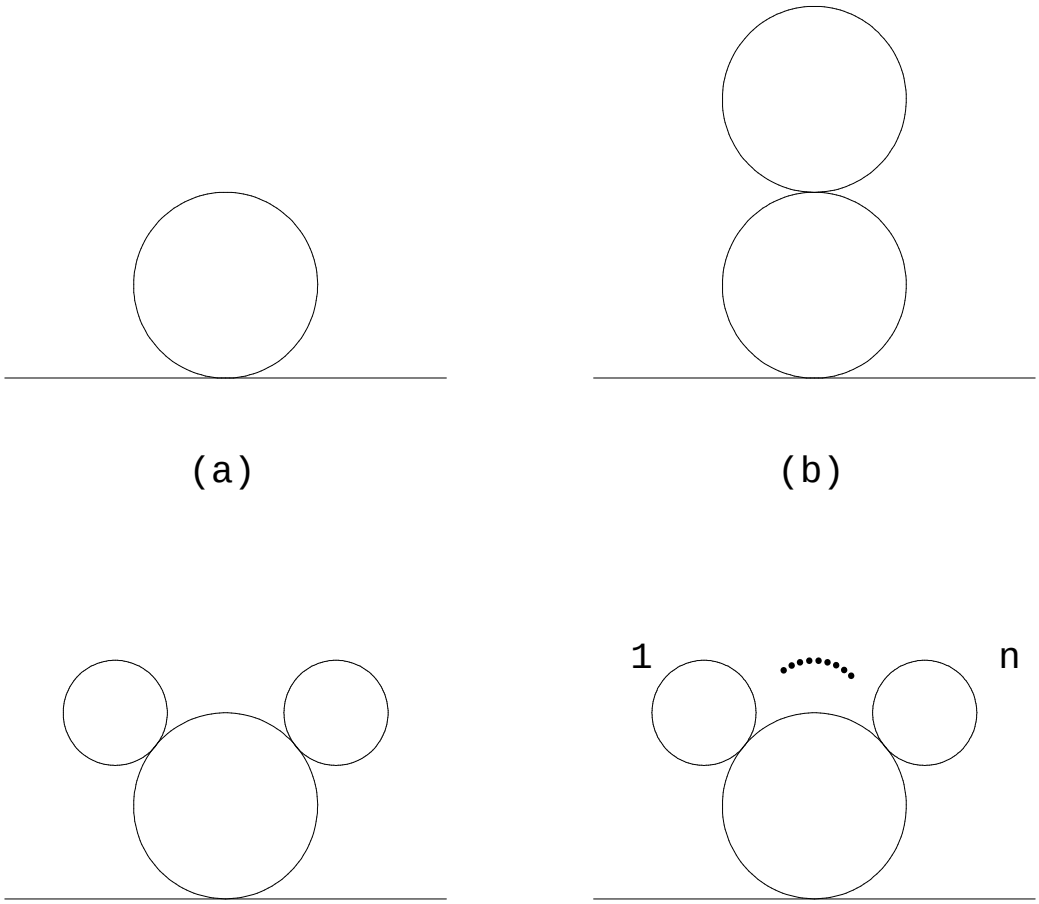

Fig. 1

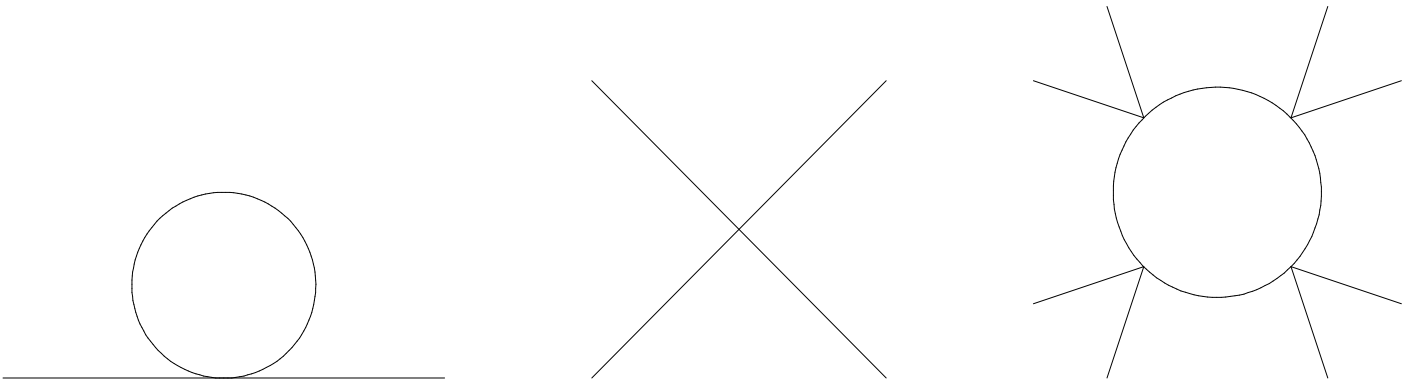

(a) (b) (c)

Fig. 2

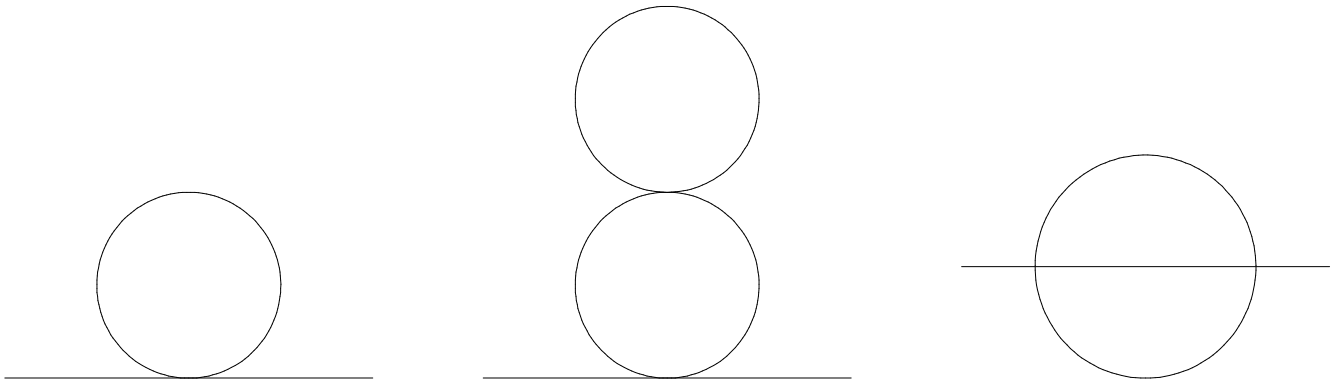

Fig. 3

Fig. 4

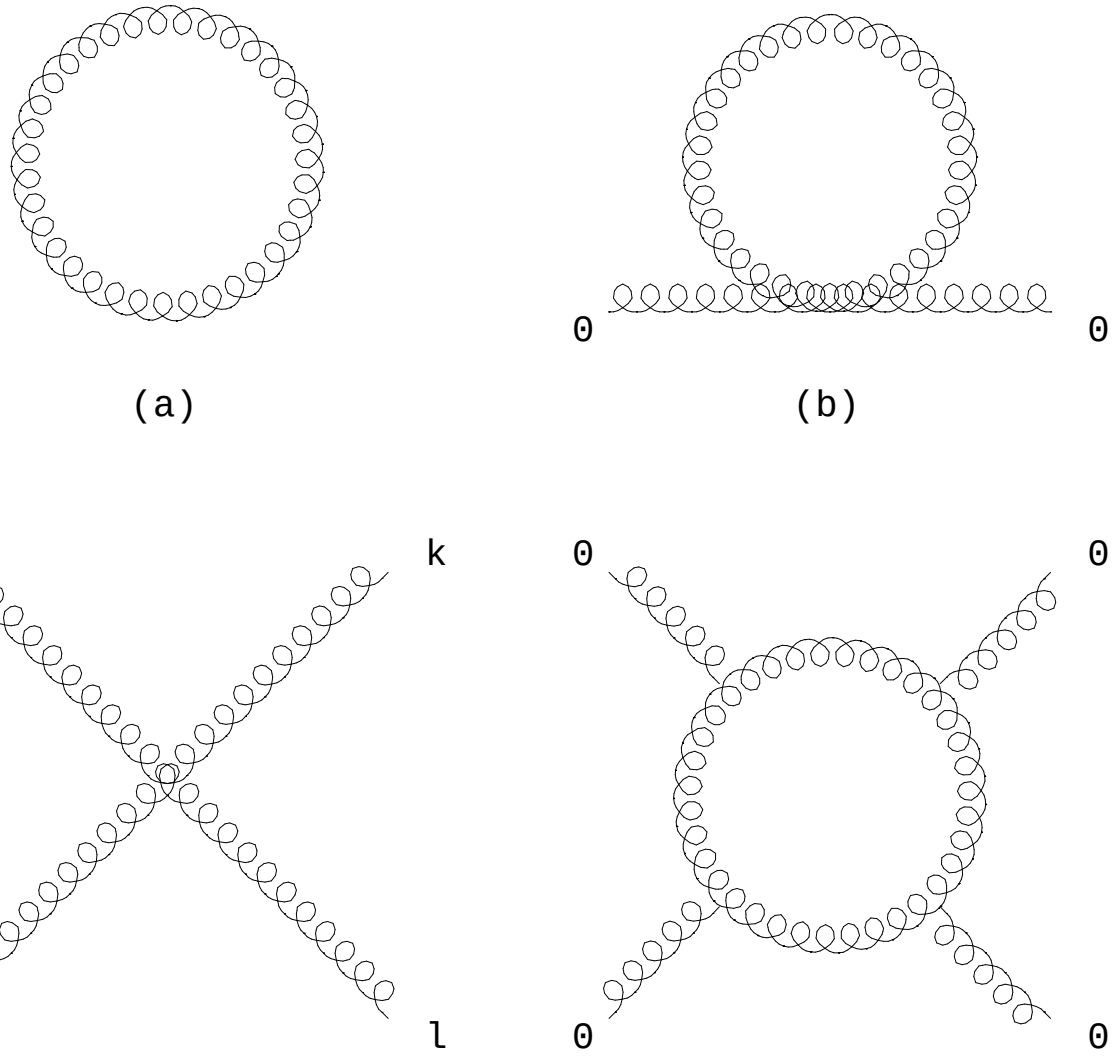

Fig. 5

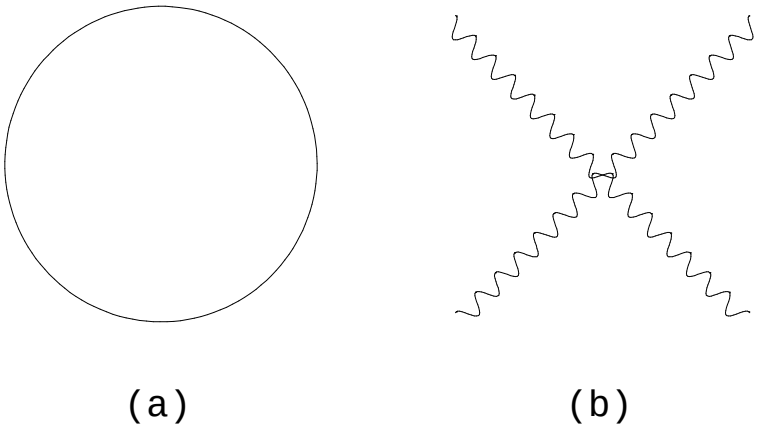

Fig. 6

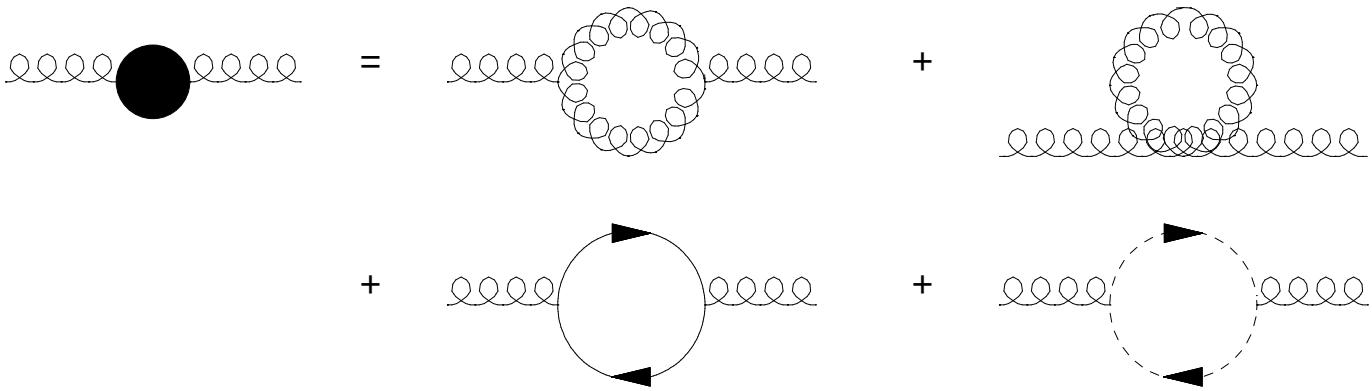

Fig. 7

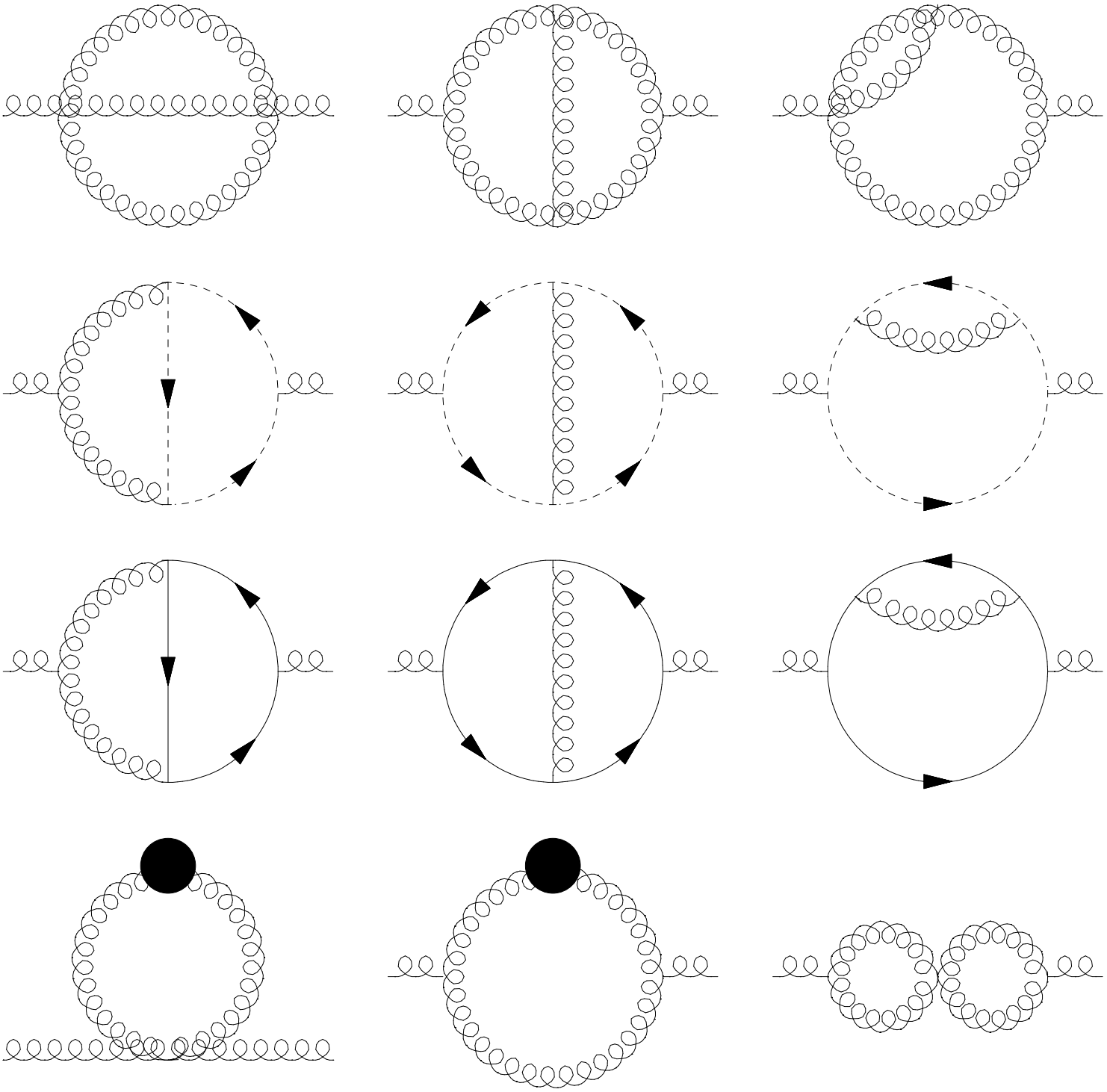

Fig.8

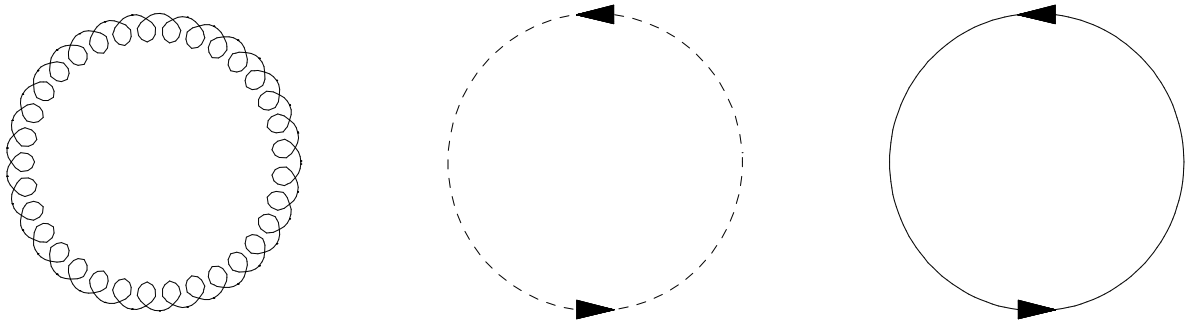

Fig. 9

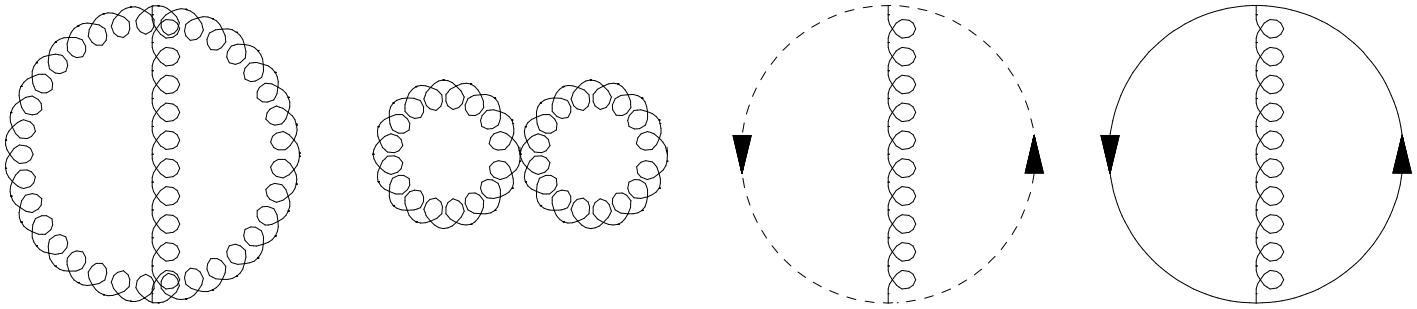

Fig. 10

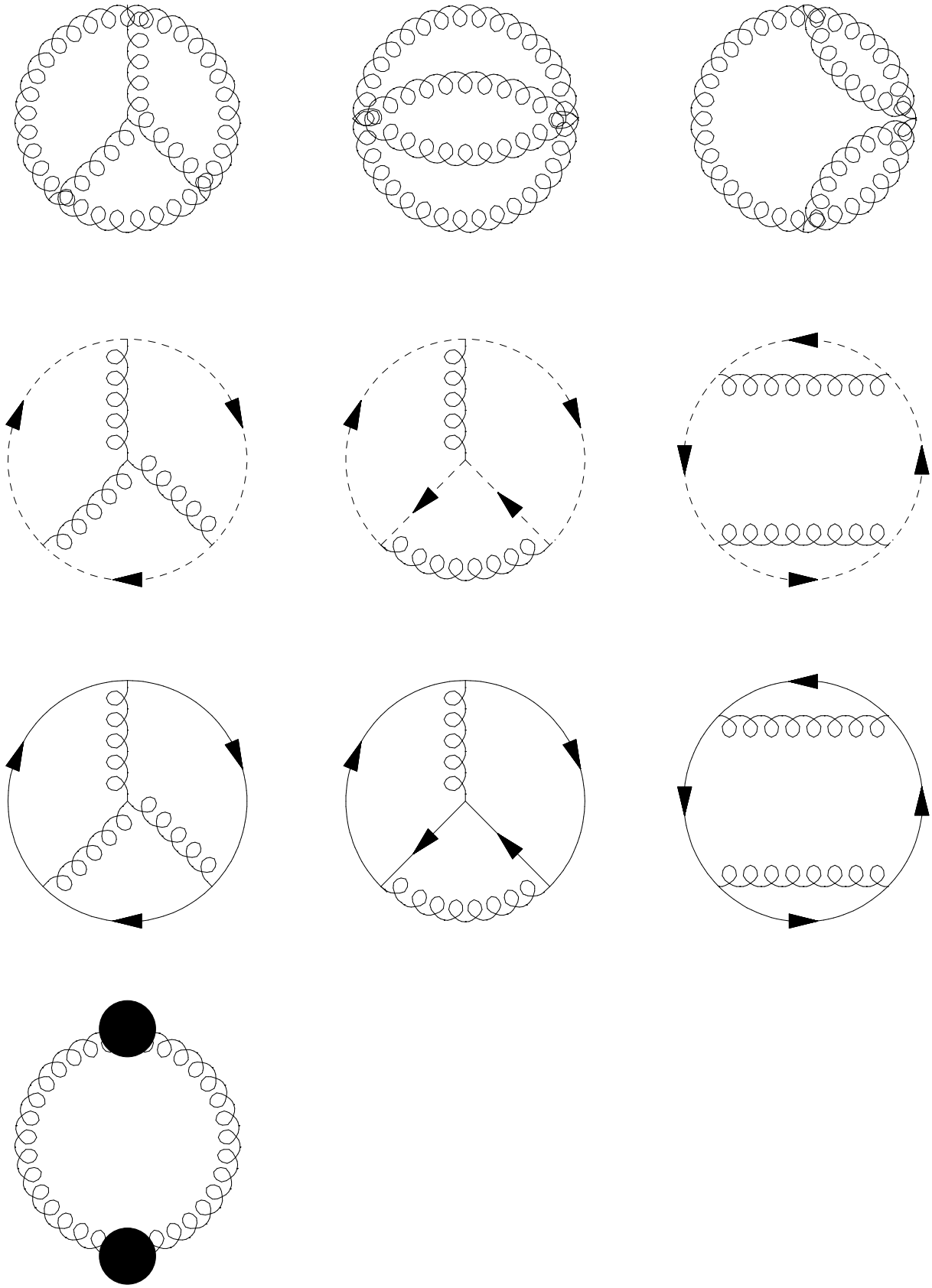

Fig. 11

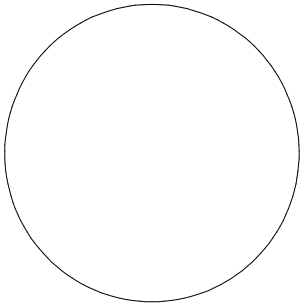

Fig. 12

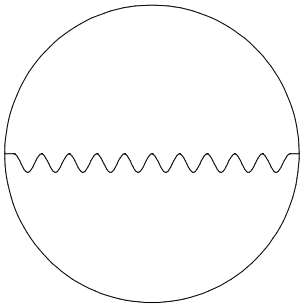

Fig. 13

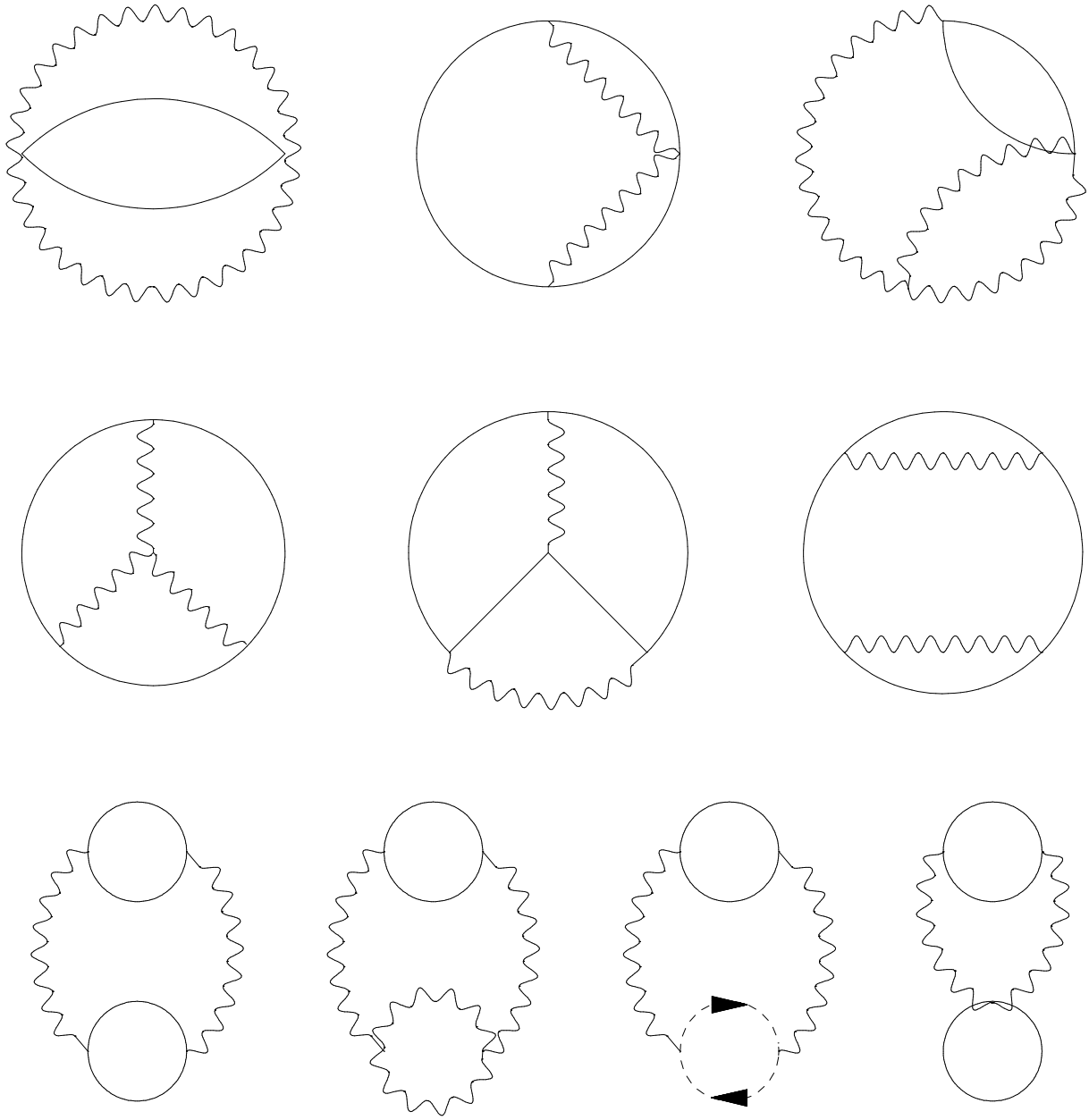

Fig. 14

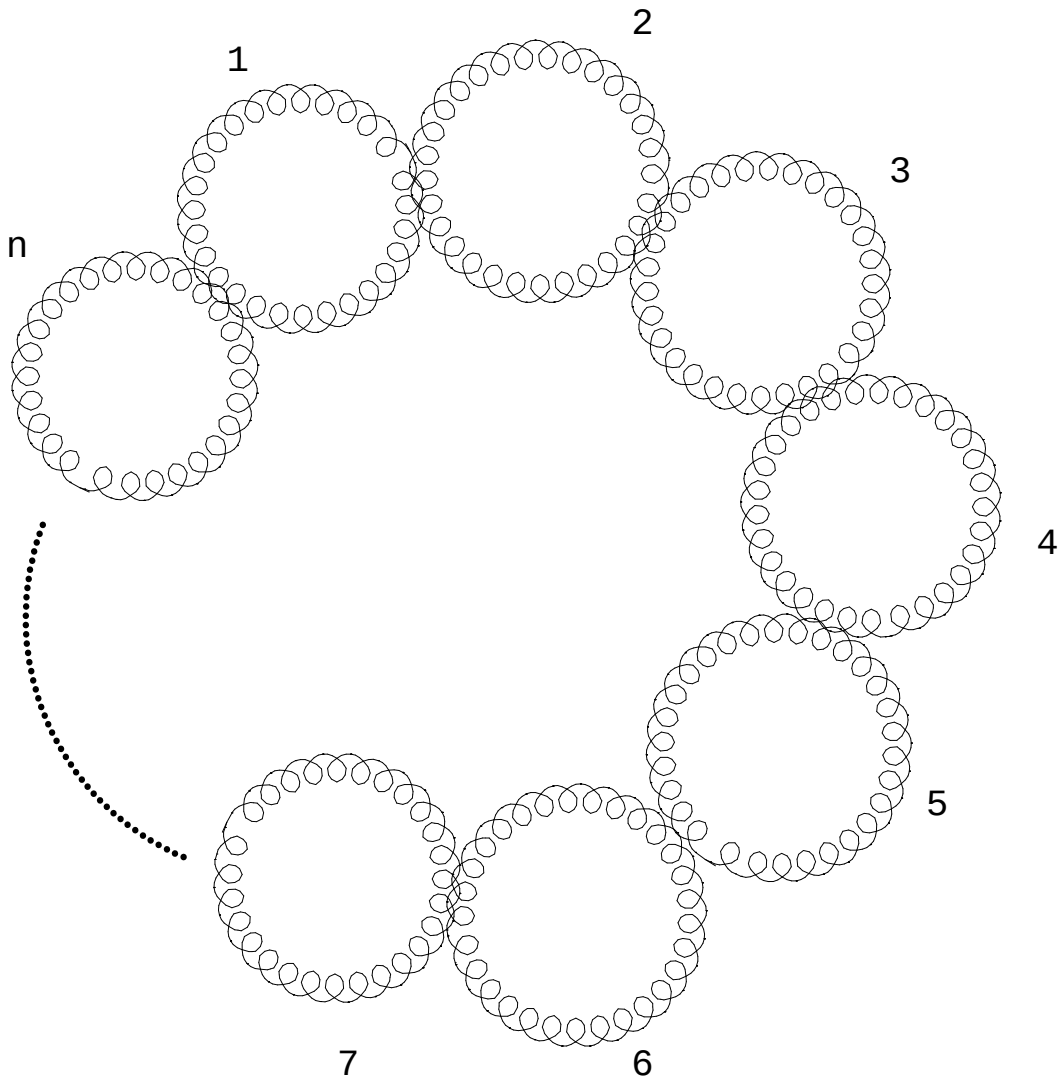

Fig. 15